T.R.

GEBZE TECHNICAL UNIVERSITY

INSTITUTE OF BIOTECHNOLOGY

DEVELOPMENT OF Ca DOPED ZnO THIN FILMS FOR OPTICAL BIOSENSORS USED IN BIOMEDICAL APPLICATIONS

GAMZE SEKİCEK

A THESIS SUBMITTED FOR THE DEGREE OF MASTER OF SCIENCE

DEPARTMENT OF BIOTECHNOLOGY

THESIS SUPERVISOR

ASST. PROF. ZEHRA BANU BAHŞİ ORAL

GEBZE

2022

T.R.

GEBZE TECHNICAL UNIVERSITY

INSTITUTE OF BIOTECHNOLOGY

DEVELOPMENT OF Ca DOPED ZnO THIN FILMS FOR OPTICAL BIOSENSORS USED IN BIOMEDICAL APPLICATIONS

GAMZE SEKİCEK

A THESIS SUBMITTED FOR THE DEGREE OF MASTER OF SCIENCE

DEPARTMENT OF BIOTECHNOLOGY

THESIS SUPERVISOR

ASST. PROF. ZEHRA BANU BAHŞİ ORAL

GEBZE

2022

T.C.

GEBZE TEKNİK ÜNİVERSİTESİ

BİYOTEKNOLOJİ ENSTİTÜSÜ

BİYOMEDİKAL UYGULAMALARDA KULLANILAN OPTİK BİYOSENSÖRLER İÇİN Ca KATKILI ZnO İNCE FİLMLERİN GELİŞTİRİLMESİ

GAMZE SEKİCEK

YÜKSEK LİSANS TEZİ

BİYOTEKNOLOJİ ANABİLİM DALI

DANIŞMANI

DR. ÖĞR. ÜYESİ ZEHRA BANU BAHŞİ ORAL

GEBZE

2022

GEBZE TEKNİK ÜNİVERSİTESİ	**YÜKSEK LİSANS JÜRİ ONAY FORMU**

GTÜ Biyoteknoloji Enstitüsü Yönetim Kurulu'nun 27/12/2021 tarih ve 2021/28 sayılı kararıyla oluşturulan jüri tarafından 28/12/2021 tarihinde tez savunma sınavı yapılan Gamze SEKİCEK'in tez çalışması Biyoteknoloji Anabilim Dalında YÜKSEK LİSANS tezi olarak kabul edilmiştir.

JÜRİ

ÜYE (TEZ DANIŞMANI)	: Dr. Öğr. Üyesi Zehra Banu BAHŞİ ORAL
ÜYE	: Prof. Dr. Işıl AKSAN KURNAZ
ÜYE	: Dr. Öğr. Üyesi Eftal ŞEHİRLİ

ONAY

Gebze Teknik Üniversitesi Fen Bilimleri Enstitüsü Yönetim Kurulu'nun

...…/……/…… tarih ve ……/…..... sayılı kararı.

SUMMARY

Optical biosensors have great potential in a variety of fields, including healthcare and biomedical industry. Nanomaterials are known to be an excellent component as a biorecognition layer for biosensor applications. Thin films based on zinc oxide (ZnO) are promising materials for sensor surfaces due to their good biocompatibility for binding biological molecules, large surface area and improved optical properties. From past to present, the chemical bisphenol A (BPA) has been linked to various health problems and needs to be detected.

In this study, ZnO and calcium (Ca) doped ZnO thin films were fabricated by sol-gel dip and spin coating methods. The thermal properties of the ZnO powder were investigated by thermogravimetric/differential thermal analysis (TG/DTA). X-ray diffraction (XRD), scanning electron microscopy (SEM) and Atomic Force Microscopy (AFM) were used to characterize the microstructure and surface morphology of the thin films. The prism coupler was used to measure the refractive index of the thin films prepared by dip coating. The surface porosity ratio was calculated using Python image data analysis for all thin films. The results show that the 10% Ca doping ratio had a significant effect on the microstructural properties of the ZnO thin films and was most suitable for antibody immobilization. The aim was to immobilize bisphenol A (BPA) antibodies on the surface of Ca-doped ZnO thin films to demonstrate that the developed thin films can be used in biosensors. The UV-Vis-NIR spectrophotometer was used to study the optical properties of the thin films and used as an optical transducer to detect BPA.

Key Words: Optical Biosensor, Thin Film, Ca doped ZnO, Sol-gel

ÖZET

Optik biyosensörler, sağlık ve biyomedikal endüstrisi de dahil olmak üzere çeşitli alanlarda büyük potansiyele sahiptir. Nanomalzemelerin, biyosensör uygulamaları için bir biyotanıma katmanı olarak mükemmel bir bileşen olduğu bilinmektedir. Çinko oksit (ZnO) bazlı ince filmler, biyolojik molekülleri bağlamak için iyi biyouyumlulukları, geniş yüzey alanı ve geliştirilmiş optik özellikleri nedeniyle sensör yüzeyleri için umut verici malzemelerdir. Geçmişten günümüze kimyasal bisfenol A (BPA) çeşitli sağlık sorunlarıyla ilişkilendirilmiştir ve tespit edilmesi gerekmektedir.

Bu çalışmada, sol-jel daldırma ve döndürmeli kaplama yöntemleri ile ZnO ve kalsiyum (Ca) katkılı ZnO ince filmler üretilmiştir. ZnO tozunun termal özellikleri termogravimetrik/diferansiyel termal analiz (TG/DTA) ile araştırılmıştır. İnce filmlerin mikro yapısını ve yüzey morfolojisini karakterize etmek için X-ışını kırınımı (XRD), taramalı elektron mikroskobu (SEM) ve Atomik Kuvvet Mikroskobu (AFM) kullanılmıştır. Daldırma kaplama ile hazırlanan ince filmlerin kırılma indisini ölçmek için prizma kuplörü kullanılmıştır. Tüm ince filmler için Python görüntü veri analizi kullanılarak yüzey gözeneklilik oranı hesaplanmıştır. Sonuçlar, %10 Ca katkılama oranının ZnO ince filmlerin mikroyapısal özellikleri üzerinde önemli bir etkiye sahip olduğunu ve antikor immobilizasyonu için en uygun olduğunu göstermektedir. Geliştirilen ince filmlerin biyosensörlerde kullanılabileceğini göstermek için Ca katkılı ZnO ince filmlerin yüzeyinde bisfenol A (BPA) antikorlarının immobilize edilmesi amaçlanmıştır. UV-Vis-NIR spektrofotometresi, ince filmlerin optik özelliklerini incelemek için kullanılmıştır ve BPA'yı saptamak için bir optik dönüştürücü olarak kullanılmıştır.

Anahtar Kelimeler: Optik Biyosensör, İnce Film, Ca katkılı ZnO, Sol-jel

ACKNOWLEDGEMENTS

First of all, I would like to thank with a great sincerity to Asst. Prof. Zehra Banu BAHSI ORAL for her supervision, guidance and advice during the period of my research.

I would like to thank my dear laboratory colleagues Seda KOL, Onur Alp AKSAN and Mehmet SEZER for all their support, friendship and all the beautiful memories.

I would like to thank Prof. Dr. Isıl AKSAN KURNAZ for opening her laboratory and also Sedef YUSUFOĞULLARI and Mustafa Doğukan METINER for their help in antibody dilution.

I would also like to thank Assoc. Prof. Aligul BUYUKAKSOY for providing the laboratory facilities that enabled me to complete my work and for his kindness.

I would like to thank Ahmet NAZIM ve Adem ŞEN for the thin film characterizations.

I would like to thank my best friends Sahika AKDOGAN, Tugce ALKOC and Yasemin SEVEN for their friendship and moral support.

Above all, I thank all members of my family, especially my mother Hamide SEKICEK and my father Mehmet SEKICEK for their support, patience and endless love.

My very special thanks also go to my dear Kubilay TAN for his constant support, endless encouragement, patience and precious love.

TABLE of CONTENTS

LIST of ABBREVIATIONS and ACRONYMS

Abbreviations and Acronyms		Explanations
°C	:	Celsius
ρ	:	Density
β	:	Effective Index
A	:	Absorbance
Ba	:	Barium
Be	:	Beryllium
BPA	:	Bisphenol A
Ca	:	Calcium
$Ca(CH_3COO)_2$	:	Calcium Acetate Hydrate
CNTs	:	Carbon Nanotubes
APTES	:	3-aminopropyl-triethoxysilane
DNA	:	Deoxyribonucleic Acid
DI	:	Deionized Water
$Ca(CH_3COO)_2$	:	Diethanolamine
dsDNA	:	Double-Stranded DNA
EDCs	:	Endocrine Disrupting Chemicals
C_2H_5OH	:	Ethanol
FLISA	:	Fluorescence-Linked Immunoassay
Au	:	Gold
IUPAC	:	International Union of Pure and Applied Chemistry
Fe	:	Iron
LOD	:	Limit of Detection
LSPR	:	Localized Surface Plasmon Resonance
Mg	:	Magnesium
Mn	:	Manganese
MBE	:	Molecular Beam Epitaxy
mm	:	Millimeter
μm	:	Micrometer

N	:	Number of Analyte Molecules
nm	:	Nanometer
PEC	:	Photoelectrochemical
PC	:	Polycarbonate
PAHs	:	Polycyclic Aromatic Hydrocarbons
PCR	:	Polymerase Chain Reaction
QDs	:	Quantum Dots
QCM	:	Quartz Crystal Microbalance
RBC	:	Red Blood Cells
RNA	:	Ribonucleic Acid
Ag	:	Silver
ssDNA	:	Single-Stranded DNA
SEM	:	Scanning Electron Microscopy
Sr	:	Strontium
SAW	:	Surface Acoustic Wave
SERs	:	Surface-Enhanced Raman Scattering
SPR	:	Surface Plasmon Resonance
T	:	Transmittance
V	:	Volume
Zn	:	Zinc
ZnO	:	Zinc Oxide
$Zn(CH_3COO)_2 \cdot 2H_2O$	:	Zinc Acetate Dihydrate
H_2O	:	Water
WBC	:	White Blood Cells
XRD	:	X-Ray Diffraction

LIST of FIGURES

LIST of TABLES

1. INTRODUCTION

Biosensors are nowadays widely used in biomedical diagnosis to observe the progression of treatment and disease, as well as in a variety of other biotechnological fields such as environmental monitoring, food safety, drug discovery, forensics, agriculture, and many others [1],[2],[3]. A biosensor is generally defined as an analytical device that combines a biological recognition system (bioreceptor and biorecognition layer) and a physiochemical transducer to detect target molecules by converting a biological signal into a measurable output signal [4]. The first biosensor which is composed of an oxygen electrode was discovered for measuring glucose levels in the 1962 by Clark and Lyons [4],[5],[6]. Since the development of the first biosensor, the increasing need for biosensors has led researchers to develop more and more new technologies, and today the biosensor industry is worth billions of dollars [3],[4],[7].

Optical biosensors are one of the most widely reported biosensor types. These devices have several advantages over traditional analytical techniques, including the ability to detect a wide range of biological and chemical substances directly, in real time, and without the use of labels. Optical biosensors detect changes in light properties such as refractive index, absorption, fluorescence, or light scattering as a result of an analyte-receptor interaction [8],[9]. A biorecognition layer is required to integrate the sensing biomolecules into the system. A suitable biorecognition layer helps biomolecules immobilize with retained or enhanced activity and promotes signal transduction [10]. Several studies have shown the importance of nanostructured materials as biorecognition layers for biosensors because they have a large surface area, which increases the surface-to-volume ratio and facilitates the attachment of biomolecules to the surface [11],[12],[13]. Zinc oxide is a unique n-type semiconducting material with a wide bandgap of 3.37 eV, non-toxic, bio-safe, and biocompatible, and has a high isoelectric point of 9.5, making it a promising biomaterial as biorecognition layer for biosensor applications [14]. ZnO thin films and nanostructures have recently received a lot of attention as a potential biorecognition layer. Furthermore, ZnO thin films and nanostructures enhance sensing characteristics of biosensors by improving biomolecule attachment and increasing the surface to volume ratio. Grain size changes in ZnO thin films are caused by doping group II

elements such as Be, Mg, Ca, Sr, and Ba [15]. In this thesis study, it is aimed to find the effect of Ca doping on the structure of ZnO thin films that could be used in biosensors. For this reason, (at 10%) Ca doped ZnO thin films were produced by using sol-gel dip coating and spin coating methods. Characterization of the films was determined by using XRD, SEM and AFM. After characterization, Bisphenol A (BPA) was detected by using antibody immobilized 10% Ca doped ZnO thin films via sol-gel spin coating as a biorecognition system in optical biosensors. UV–Vis-NIR spectrophotometer (Shimadzu, UV-3600i Plus) as an optical transducer was used for the measurement of optical properties of thin films and BPA detection.

2. BIOSENSORS

Biosensors are devices that consist of a biological recognition element (bioreceptor) and a physical or chemical transducer to detect an analyte by producing a signal that can be measured. Biosensors are integrated receptor–transducer devices that can provide selective quantitative or semiquantitative analytical information using a biorecognition element, according to IUPAC nomenclature [16],[17]. A typical biosensor usually comprises of a bioreceptor, transducer component and electronic system which amplifies the signal and records the signal for data presentation [17]. Fig. 2.1 shows a schematic of a biosensor. It also has a lot of uses in the food industry, clinical diagnostics, and a lot of other fields where precise and reliable analyses are needed. Moreover, biosensors overcome some disadvantages of conventional analytical techniques such as the need of much time, centralized laboratories, tedious work and large, expensive devices [18],[19]. Several biosensor elements and devices have been developed over the last few decades. Biosensors are successfully used for disease detection, prevention, rehabilitation, patient health monitoring, and health management [20]. Due to advantages such as high selectivity and sensitivity, potential miniaturization, portability, low cost, and rapid response, biosensors have recently gained traction in a variety of fields, including clinical and biomedical applications [21].

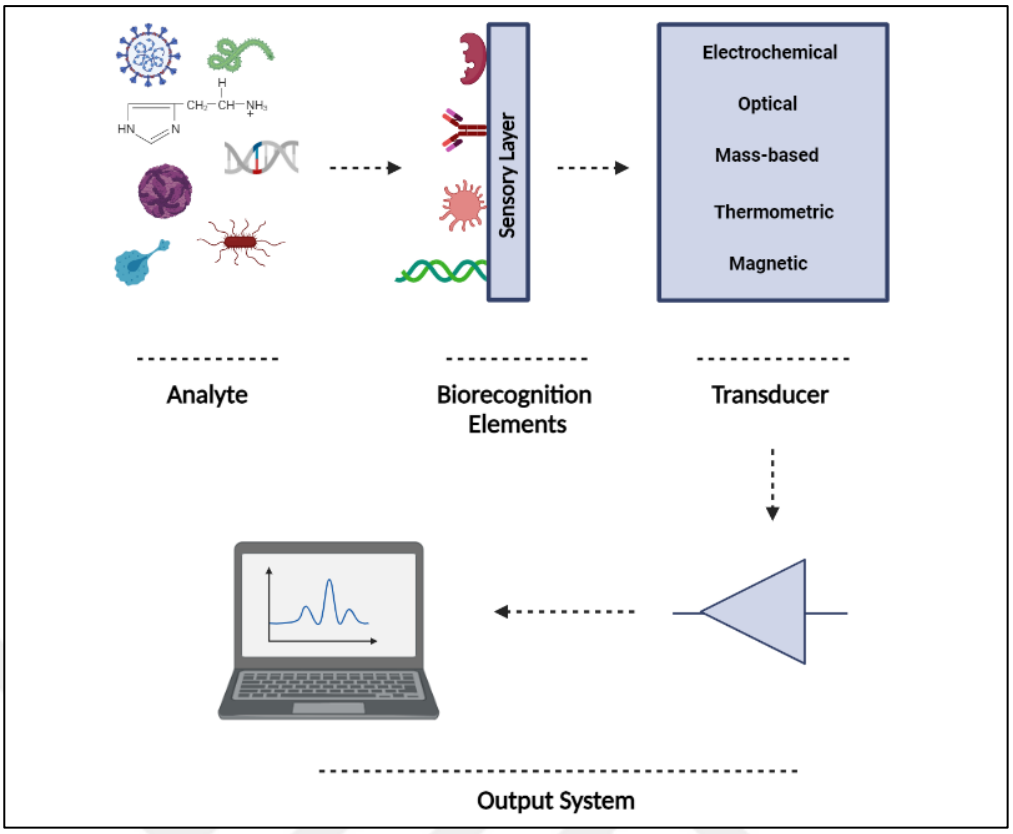

Figure 2.1: Schematic representation of biosensors

3. CHARACTERISTICS of BIOSENSORS

There are certain qualities that any ideal biosensor should possess. The optimization of these qualities is reflected in the performance of the biosensor [22].

3.1. Sensitivity

Sensitivity is defined as the minimum amount of analyte that can be detected by a biosensor and can be evaluated with the limit of detection (LOD) values. In addition, sensitivity is a function of several factors involved in biosensor design and operation. The geometry of the transducer surface, the surface density of the immobilized coating, the molecular diffusivity of the free analyte in the sample solution, and the reaction kinetics are important factors in sensitivity. Increasing the surface area to volume ratio is directly related to improving the sensitivity of biosensors. [23].

3.2. Selectivity

Selectivity is the ability to discriminate the target molecule (analyte) in the sample containing other molecules. The selectivity is mostly important in biological samples where the target concentration can be much lower than the concentration of existing other biomolecules in the sample. The interaction of an antigen with an antibody is the best example of selectivity. Antibodies are commonly used as bioreceptors, and they are immobilized on the surface of transducer. A solution containing the antigen (usually a saline buffer) is then introduced to the transducer, where the antibodies bind exclusively to the antigens. This ensures that the device is a sensor specific to the analyte to be detected [24].

3.3. Response Time

Response time is another important performance of biosensors. It is defined as the minimum time required for a biosensor to detect a sufficient amount of biomolecules to identify an analyte. Critical to this process are the density of the target

biomolecules and the physical diffusion of these biomolecules to the sensor surface. Response time is determined by the diffusion of the biomolecules (target molecules) through the solution and their subsequent capture at the sensor surface [25]. Dak p. et. al. explained that response time (ts) depends on the concentration of analyte in the sample by following equation (Eq.3.1) [25];

$$\rho = \frac{N}{V} \tag{3.1}$$

Here, ρ, N and V are the analyte concentration, number of analyte molecules and sample volume, respectively. At very low of analyte concentrations (ρ), the response time (ts) will take long. ρ can be increased by increasing N according to this equation. Thus, they brought up the expensive and complex instrumentation techniques such as polymerase chain reaction (PCR) or commercial assays. Moreover, these techniques require long processing time and trained personnel compared to biosensors.

3.4. Reproducibility

The ability of a biosensor to produce identical responses for a duplicated set of experiments is known as reproducibility. It is distinguished by precision (consistent results when the sample is measured multiple times) and accuracy (the degree of closeness between measured value and the true value). Reproducible signals ensure high reliability and robustness when inferring from a response of biosensors [26].

3.5. Stability

In biosensor applications that require continuous monitoring, one of the most important features is stability. Stability refers to the degree of vulnerability to environmental perturbations both inside and outside the biosensing device. The affinity of the bioreceptor (the rate of binding of the analyte to the bioreceptor) and the degradation of the bioreceptor over time are two factors that influence stability. For instance; temperature can affect the performance of transducers and electronics, which can affect a stability of biosensors [2].

3.6. Linearity

The accuracy of the measured response is described by the property of linearity (for a collection of measurements with varied analyte concentrations) to a straight line, mathematically defined as Eq.3.2, where c is the analyte concentration, y is the output signal, and m is the sensitivity of biosensor. The linearity of the biosensor is related to the resolution of the biosensor and the range of analyte concentrations under test. The resolution of a biosensor is defined as the lowest change in analyte concentration required to cause a change in the response of the biosensor. Most biosensor applications require not only analyte detection but also monitoring of analyte concentrations over a wide working range, hence a high resolution is necessary depending on the application [27].

$$y = m.c \tag{3.2}$$

4. CLASSIFICATION of BIOSENSORS

Biosensors are generally classified according to the type of transducer and the type of bioreceptor or a combination of the two [28]. Transduction can be optical, electrochemical, thermometric, piezoelectric, magnetic, or micromechanical, and a bioreceptor can be a tissue, microorganism, organelle, cell, enzyme, antibody, nucleic acid, or bio-mimic [29].

4.1. Transducer based Biosensors

Signal transduction in biosensors is typically accomplished using one or more of the following five methods: i) optical, ii) electrochemical, iii) mass-based, iv) thermometric, and v) magnetic. The most widely used and sensitive biosensor techniques are electrochemical and optical, while mass-based and thermometric methods are also important in biosensing. The underlying principles of signal detection for biosensors used in the biomedical field are briefly discussed in this section.

4.1.1. Optical Biosensors

During a biochemical reaction, an optical biosensor measures the amount of light absorbed or emitted. The signal is based on optical properties such as absorption, fluorescence/phosphorescence, bio/chemiluminescence, reflectance, light scattering, and refractive index in optical biosensors (Fig. 4.1) [30]. Optical biosensors are generally divided into two types: label-free and label-based detection. The observed signal is generated directly by the analyte and transducer interacting on-site in label-free detection. Label-free biosensors use biophysical properties such as molecular weight, refractive index (e.g. surface plasmon resonance), and charge to detect the presence and/or activity of molecules of interest. A label is used in label-based sensing, and an optical signal is generated by a colorimetric, fluorescent, or luminescent device [31]. Label-free detection methods are available using biosensors based on SPR, ellipsometry, reflectometry, interferometry, or photoluminescence. Labeled based biosensors are based on fluorescence, SERS, photoluminescence quantum dots (used as labels) and other optical techniques.

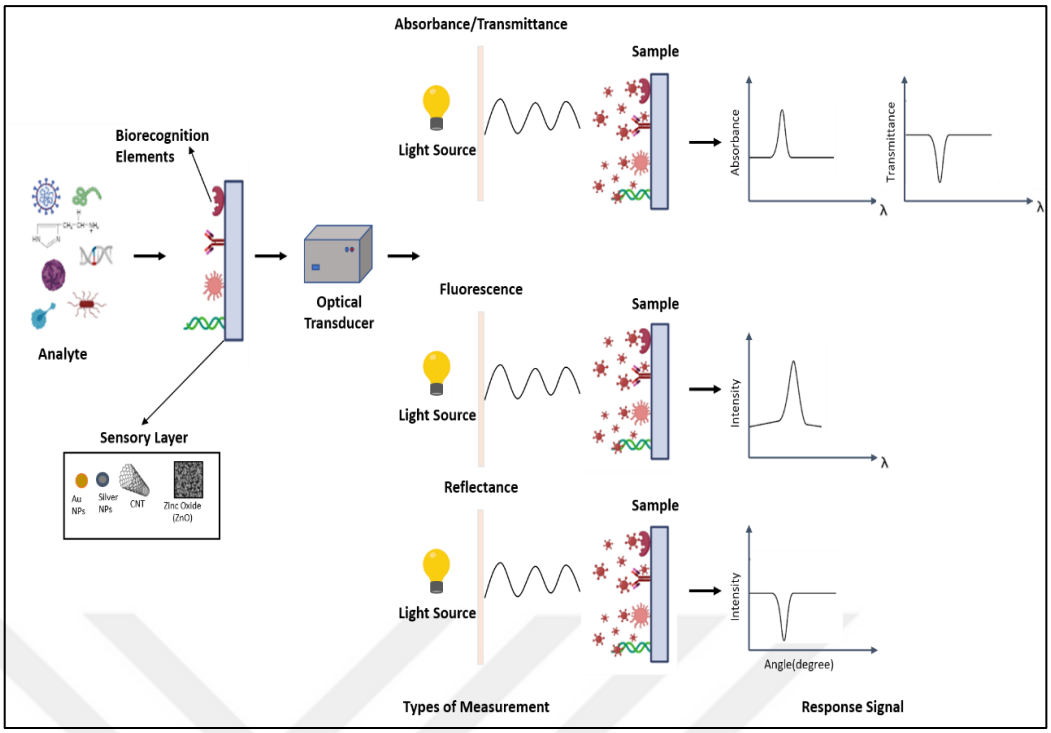

Figure 4.1: Optical signal transduction

Among the various optical biosensor techniques, surface plasmon resonance (SPR) sensors are suitable for different classes of analytes of clinical interest. A surface plasmon (SP) wave detects a change in refractive index caused by molecular interactions on a metal surface, making SPR the most widely used and well-known technology. When photons from an incoming wave collide with electrons on the metal surface, SPs are formed. A SP wave is formed when plasmons propagate parallel to the metal surface. The most commonly used coupling structures are prism couplers, waveguide couplers, grating couplers and fiber couplers [32]. SPR sensing can be used to detect antibodies, proteins, enzymes, medicines, tiny molecules, peptides, nucleic acids, and viruses in a variety of clinical assays. Sensing can be performed in a broad range of biofluids such as serum, urine, plasma, white blood cells (WBC), red blood cells (RBC), whole blood, stools, synovial fluid, cerebrospinal fluids, saliva [33].

While metals such as Au and Ag have been thoroughly studied and reviewed as plasmonic materials, novel materials with two-dimensional plasmons, such as graphene and polymers, are currently being investigated as prospective plasmonic materials in biosensors [34]. Metal nanoparticle-based localized surface plasmon resonance (LSPR) sensors are an effective platform for biomolecule detection, and the sensing technique has the advantage of being easily multiplexed to enable the electric

field at the nanoscale around the metal nanoparticles [35]. Material-based optical waveguide biosensors can provide rapid, sensitive and reliable alternative to next-generation, smart healthcare devices due to the excellent properties of biomaterials [36].

4.1.1.1 UV-Vis-Nir Spectrophotometer used as an Optical Transducer

UV–Vis is the most common optical characterization technique to monitor the formation of nanoparticles by observing the characteristic absorption bands [37]. Zhu et al. developed an optical sensor for antibiotic detection by UV–vis absorbance spectrometry based on surface plasmon resonance absorption property of gold nanoparticles [38]. The Uv-Vis spectroscopy measurements were also used by Que and his collaborators to develop a novel optical immunosensor for tracking antibiotic residues [39].

The optical band gap of the thin films is calculated using the relationship (Eq. 4.1) by extrapolating the linear intercept of the αhν versus hν diagrams:

$$\alpha h\nu = A(h\nu - E_g)^n \quad (4.1)$$

where hν is the incident photon energy, A is a constant that depends on the properties of the materials, Eg is the optical band gap, and n can be 1/2, 3/2, 1, 2, or 3, depending on the nature of the electronic transition. The plots of αhν versus hν are linear over a wide range of photon energies, indicating that the transitions are direct. The energy band gaps are determined by the intercepts (extrapolations) of these plots (straight lines) on the energy axis [40].

The part of light that passes through the other side of a surface or material is defined as the transmittance of light. Light can be transmitted, reflected, or absorbed as it passes through a surface or material. The ratio (Eq. 4.2) between the intensity of the incident light (I0) and the amount of light passing through the object is called the transmittance (I). The transmittance is represented by the letter T. The transmittance can be used to calculate the amount of radiation absorbed.

$$T = I_0 / I \quad (4.2)$$

The Lambert's formula was used to calculate the optical absorption coefficient α for each film. The Beer-Lambert law (also known as Beer's law) describes the relationship between transmittance (T) and absorbance (A) as shown in Eq.4.3.

$$A = -\log_{10} T \quad (4.3)$$

4.1.2. Electrochemical Biosensors

Signals derived from biochemical events such as enzyme-substrate reactions and antigen-antibody interactions are converted into electrical signals by the electrochemical biosensor (e.g., current, voltage, impedance, etc.) [41]. Electrochemical techniques (Fig. 4.2) are generally divided into three main categories of measurements: Current, Potential, and Impedance. The main electrochemical methods are potentiometry, amperometry, voltammetry, impedance spectroscopy, and conductometry [42]. The interaction between the analyte and the bioreceptor produces a measurable current (amperometric), a measurable potential or charge accumulation (potentiometric), or measurably changes the conductive properties of a medium (conductometric) between electrodes in bio-electrochemistry [43].

Potentiometric biosensors use ion-selective electrodes and ion-sensitive field-effect transistors to convert a biochemical reaction into a potential signal [44]. Recent advances in potentiometric biosensors have enabled the measurement of neurotransmitters [45], proteins [46], bacteria [47], small molecules [48], and toxins [49]. Among electrochemical biosensors, the oldest, amperometric category is based on the monitoring of electron-transfer processes which have led to the larger number of ready to- use devices in clinical diagnostics [50]. Voltammetric biosensors measure current during controlled changes in applied potential to detect an analyte. The advantages of these sensors include highly sensitive measurements and simultaneous detection of different analytes [51]. A conductometric biosensor measures the electrical conductance/resistance of an analyte (e.g., electrolyte solutions) or a medium (e.g., nanowires) as its signal changes [52]. Impedimetric biosensors can measure biomolecular interactions such as enzymatic, DNA hybridization, antigen-antibody,

and protein-protein interactions. Changes in dielectric constant or resistance can occur when a target analyte reacts with a specific bioreceptor on a sensor surface, which can then be measured by impedimetric biosensors [53].

In electrochemical biosensors, solid electrode systems and supporting substrates are usually made of metals and carbon. Metals such as platinum, gold, silver, and stainless steel have long been used as electrochemical electrodes due to their superior electrical and mechanical properties. Carbon-based nanomaterials such as carbon nanotubes (CNTs) and graphene can be used as electrode structures and have been applied to biosensors in the medical field due to their intrinsic physicochemical properties, such as large surface area, numerous functional sites, exceptional electron transfer, enhanced thermal conductivity, mechanical stability, and biocompatibility [54]. Moreover, polymers (nanosized and nanostructured polymers, molecularly imprinted polymers) and hybrid materials can be used to improve the electroanalytical performance of transducer of biosensors and to immobilize bio-recognition elements [55].

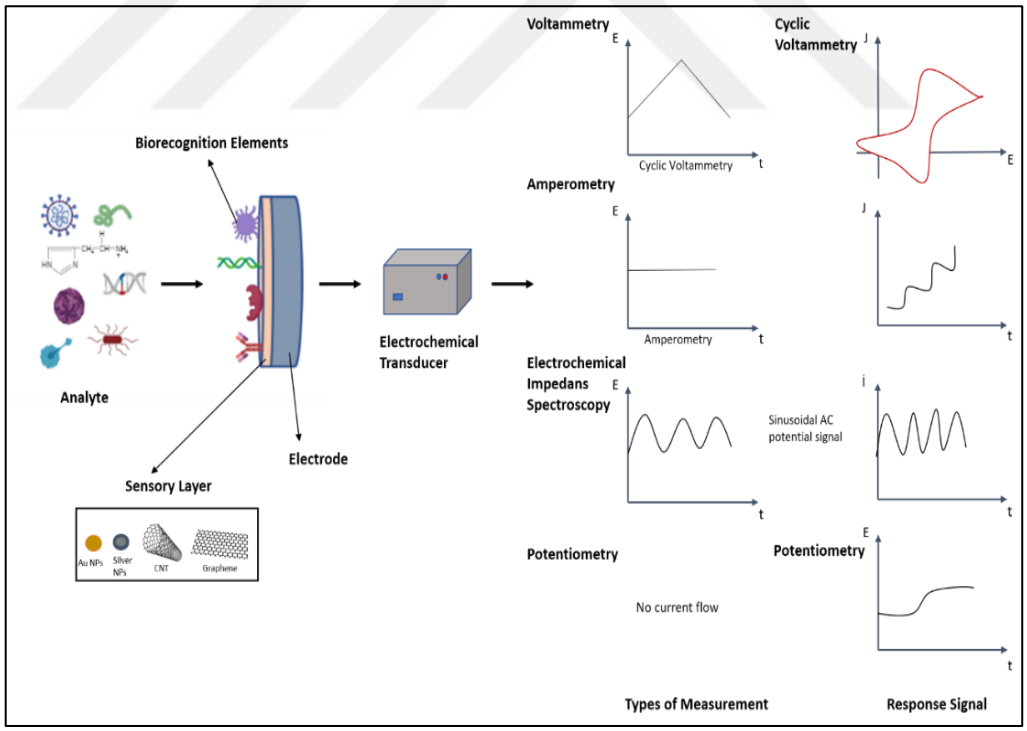

Figure 4.2: Electrochemical signal transduction

4.1.3. Thermometric Biosensors

Thermal biosensors (Fig. 4.3) detect a change in temperature of exothermic or endothermic biochemical reactions, i.e., the amount of heat energy absorbed or released during the reaction. The most common temperature sensors are thermistors and thermopiles. The thermistor is a sensitive temperature transducer that relies on changes in electrical resistance with temperature to measure absolute temperature but has limited sensitivity. The temperature difference between the two regions is measured by thermopiles, which are a series of thermocouple junctions. Metals, semiconductors, and various substrate semiconductor components can be used to make thermocouple junctions [56]. Microelectromechanical (MEMS) thermal sensors have recently been employed to monitor metabolic applications on the basis of temperature detection. MEMS technology has the advantages of low-cost miniaturized device integration and low-cost batch manufacture. The MEMS thermal biosensor has a linear range and high sensitivity, as well as a short measurement time and low power consumption, as well as improved thermal isolation, lower thermal mass, and a smaller sample volume. Multiple samples can be measured at the same time with these devices [57].

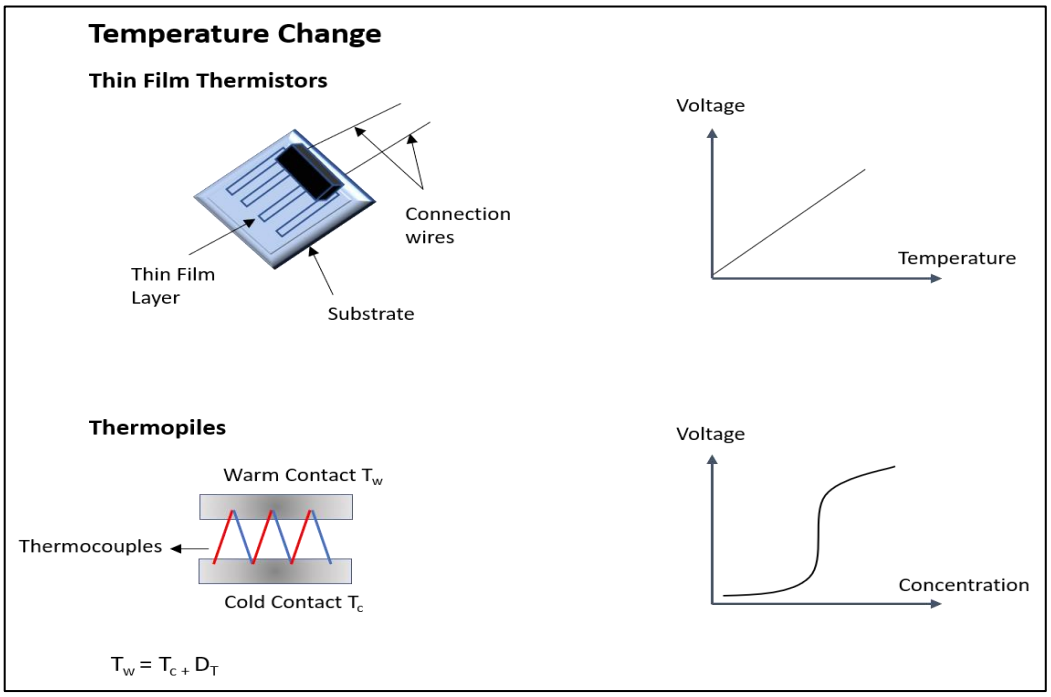

Figure 4.3: Thermometric signal transduction

4.1.4. Mechanical Biosensors

Mechanical biosensing is a useful approach to measure physical changes due to stress, deflection, or displacement of mass caused by the interaction forces and concentrations of bioreceptor and analyte [58]. Some notable mechanical biosensors are cantilever, quartz crystal microbalance (QCM) and surface acoustic wave (SAW) devices (Fig. 4.4). Cantilever sensors respond to changes in their environment or surface by bending mechanically in the nanometer range, which is easily detectable [59].

Immobilization techniques such as self-assembled monolayers, DNA hybridization, antibody-antigen interactions, and bacterial adsorption can be used to detect temperature and pH changes. They work by binding the analyte to the surface of a microscale cantilever, which is usually made of silicon. The quartz crystal microbalance is one of the best-known mechanical biosensor methods. These devices are based on piezoelectric quartz crystal resonators (like those found in watches) that allow direct electrical detection of crystal deformation. In these devices, the resonant frequency is measured and related to the mass change caused by the analyte binding to the immobilized detection layer on the crystal surface. A subclass of mechanical biosensors is called nanomechanical biosensors, which take advantage of the nanosize of at least one of their dimensions [60].

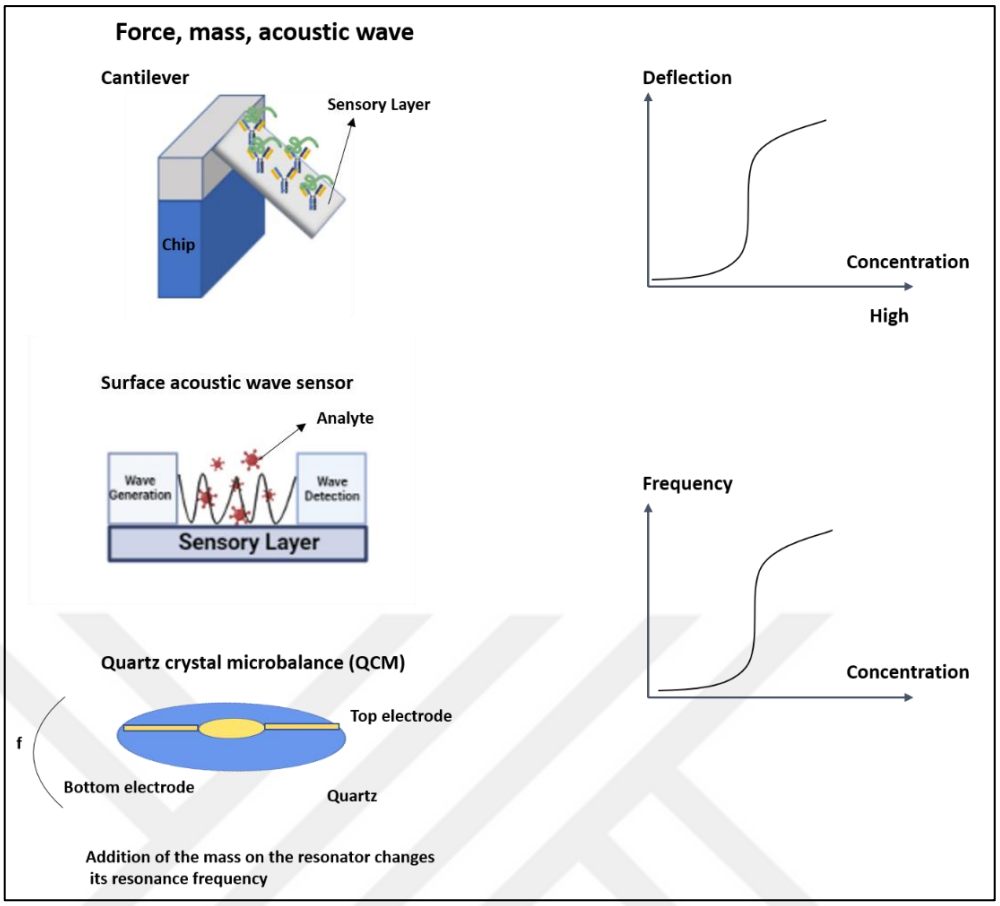

Figure 4.4: Mechanical signal transduction

4.2. Receptor Based Biosensors

According to the principle of biological recognition elements, biosensors are divided into the following categories: Enzyme sensors, Immunosensors, DNA Biosensors and Whole cell Biosensors [27].

4.2.1. Immunosensors

Most immunosensors use solid-phase immunoassays, in which antigens and antibodies are immobilized on a biorecognition layer. The antigen-antibody interaction occurs because of this reaction at the solid-liquid interface. Immunosensors are very attractive due to their high sensitivity and selectivity and the possibility to improve their affinity and selectivity by the invention of new recombinant antibodies [61].

Antibodies, also known as immunoglobins, are spherical plasma proteins with

a large size (150 kDa). They are also known as glycoproteins and are composed of two heavy chains and two light chains that form the familiar Y shape. They are produced in animals because of the immune system's response to foreign substances called antigens. Because the antibody binds the target antigen with high affinity, it can detect the analyte even when other interfering molecules are present. Antibodies, both polyclonal and monoclonal, are used to produce immunosensors. Because polyclonal antibodies can recognize different epitopes (a small area on an antigen to which a complementary antibody can specifically bind) on their target antigens, they are very sensitive but less specific, resulting in cross-reactivity. Monoclonal antibodies, on the other hand, are like monoclonal antibodies in that they are produced by the same type of immune cell and binded to the same antigen epitope, making them highly specific. Both polyclonal and monoclonal antibodies are used to produce immunosensors [26].

4.2.2. Enzymatic Biosensors

In biosensor applications, enzymes are the most commonly used bioreceptor molecules. Due to their special binding abilities as well as their catalytic activity, enzymes are often used as bioreceptors. A catalytic process enhances detection in biocatalytic detection methods. All enzymes are proteins, except for a small group of catalytic ribonucleic acid molecules. Other than their amino acid residues, some enzymes can function without chemical groups. Others require the presence of a cofactor, which can be one or more inorganic ions such as Fe^{2+}, Mg^{2+}, Mn^{2+}, or Zn^{2+}, or a more complex organic or organometallic molecule known as a coenzyme. The catalytic activity of enzymes allows for much lower detection limits than are possible with traditional binding methods [62].

Enzymes are used in biosensors because they are natural proteins that catalyze the conversion of a particular substrate molecule into a product while remaining unaffected by the reaction. Just as a key fits a lock, the enzyme recognizes a specific target analyte. Enzymes are more selective and sensitive than chemical processes, act rapidly compared to other biological sensors, and can be used in conjunction with a variety of transduction pathways. The mechanisms of action of these bioreceptors could compose of converting the analyte to a sensor-detectable product, detecting an analyte that acts as an enzyme inhibitor or activator, or evaluating the change in

enzyme properties as a result of interaction with the analyte [26].

4.2.3. Nucleic Acid-based Biosensors

Hybridization of DNA or RNA is another process of biorecognition. Nucleic acid sequencing has been used for certain diagnostic applications since early 1953, and it continues to expand. The highly specific affinity binding process between two single-stranded DNA chains (ssDNA) is used to generate double-stranded DNA (dsDNA) in nucleic acid-based biosensors that use nucleic acids as a biological recognition element [63]. Aptamers are single-stranded DNA (ssDNA) or RNA sequences of less than 100 nucleotides. Aptamers fold into a novel 3D arrangement due to the unique intramolecular interactions between these nucleotides [64].

The detection of specific DNA fragments by hybridization with a complementary strand has piqued interest due to its importance in the early diagnosis of diseases such as cancer, hypercholesterolemia, and others. This progress was largely made possible by the decoding of the human genome. Optical detection of fluorescently labelled oligonucleotides is a popular transduction principle. Array techniques can allow parallel analysis of large numbers of DNA fragments, leading to biochips or DNA chips. Despite the dominance of optical systems, electrochemical detection is showing great promise. New developments include mediated guanine oxidation in DNA, amplification of the hybridization event via enzyme labeling-impedance analysis, electron transport through the DNA double helix, and voltametric detection of redox intercalators [61].

4.2.4. Whole Cell Biosensors

Cell-based sensors are biosensors that use a living cell as a biospecific sensing component and rely on the living cell's ability to detect intracellular and extracellular microenvironmental conditions and physiological parameters and produce a response through cooperation between the jolt and the cell. Microorganisms, such as parasites and microscopic organisms, can be used as biosensors to detect specific atoms or the "state" of the environment as a whole [65].

Microbial biosensors based on luminescent reporter genes are used in a variety

of medical applications. Using either prokaryotic or eukaryotic cells, a genetically engineered whole-cell microbial biosensor detects chemical composition, toxicity, carcinogenicity, and mutagenicity in real time at a low cost. [28].

In general, a living cell-based biosensor is a type of biosensor that contain materials being removed from living creatures. The recognition of this biosensor's farthest reaches is mostly influenced by normal natural settings in which the cell can survive for long periods of time, which necessitates the regulation of physical and synthetic parameters of condition. However, the main constraint with cell-based biosensors is the cell's security, which is dependent on a variety of factors such as disinfection, lifetime, biocompatibility, and so on. Another issue that characterizes the success of a cell-based sensor is particle selectivity, in which a cell-based sensor has low microbiological sensor selectivity because to the multireceptor conduct of the cells. They can have a longer lifetime than enzymatic sensors and are substantially less expensive because dynamic cells don’t need to be contained [66].

5. IMMOBILIZATION TECHNIQUES

Combining the bioreceptors with the sensory layer to form a functioning interface is one of the most complicated tasks in biosensor design [67]. Immobilization of biomolecules on the sensor surface is a crucial step in this process. However, biomolecules cannot be immobilized directly on the surface of a biorecognition layer because they are very sensitive to their environment and can denature rapidly as a result of changes in their environment [68]. Biomolecules are usually immobilized in artificial microenvironments where they are exposed to interactions that are not present in their natural environment. In addition to preserving the conformation and biological activity of the biomolecule, the immobilization technique must ensure that the active site of the biomolecule is accessible to the target analyte and other molecules involved in biorecognition event. To achieve efficient signal transduction, there must be close proximity between the biological component and the transducer. Therefore, the choice of immobilization technique can affect a variety of biosensor properties, including sensitivity, selectivity, stability, repeatability, response time, and durability of the biosensor [69].

During the immobilization process, in addition to maintaining stability and bioactivity, it is most important that the active site remain accessible to the targets. An appropriate immobilization technique must be rapid and sufficient and must not result in percolation of the biomolecule. The size of the biomolecule, working surface, polarity, shape, presence of functional groups, and storage conditions are all critical factors that can affect immobilization. The chemical and physicochemical properties of the transducer surface also affect immobilization. There are numerous methods for immobilization of biomolecules. The most commonly used immobilization techniques are adsorption, covalent binding, crosslinking, entrapment, and affinity binding [70].

5.1. Adsorption

Adsorption is the simplest technique for immobilizing bioreceptors on the surface of the transducer by reversible surface interaction between the bioreceptor and the surface. The forces involved in this interaction are weak forces such as van der Waals forces, ionic bonds, hydrogen bonds and hydrophobic interactions. In this

technique, the biorecognition layer to be immobilized is placed in contact for an appropriate period of time with a solution containing the solubilized bioreceptor at an optimal pH, ion concentration, and other parameters for adsorption to occur. The unbound bioreceptor molecules are removed from the surface by washing with an appropriate buffer solution. Since adsorption does not involve chemical changes in the bioreceptor molecule or surface, the activity of the bioreceptor (native conformation) can be maintained during immobilization. This technique is simple, inexpensive and does not harm the bioreceptor. However, the disadvantage of this technique is that the immobilized bioreceptor can be desorbed or leached when the pH, ionic strength, temperature, or polarity of the solvent is changed because only weak forces are involved in immobilization. In this technique, desorption or leaching can be observed under changing conditions of pH, ionic strength, temperature or polarity of the solvent as only weak forces are used to achieve the immobilization process. To overcome these drawbacks, many strategies have been developed, of which immobilization on three-dimensional surfaces and/or porous structures of the matrix is widely used [71].

5.2. Covalent Binding

The most common type of immobilization is the formation of covalent bonds between the sensor surface and the bioreceptors. The functional groups of the bioreceptors, such as amine, hydroxyl, carboxyl, aldehyde, and sulfhydryl, are used for the covalent bonds with the solid transducer surfaces. Covalent immobilization is usually performed in two steps for antibody or enzyme binding. The first step is to activate the surface with linker molecules (also called carriers) such as glutaraldehyde or carbodiimide, which act as a covalent linker between the bioreceptor and the surface. After the formation of a covalent bond between the activated substrate and the bioreceptor molecule, the second step is the addition of the bioreceptor [72]. These linker/carrier molecules are composed of ideal functional groups such as hydroxyl groups that assist in the formation of covalent bonds. Moreover, their ability to form hydrogen bonds with water ensures the maintenance of a hydrophilic environment that favors the stability of the bioreceptor/enzyme. The position and homogeneity of the carrier molecules on the surface can be controlled as they form a self-assembled monolayer (SAM). This process lends itself to controlled homogeneity of the

immobilized bioreceptor on the surface, unlike adsorption. The leaching problem of bioreceptors could be solved by immobilizing them through covalent bonds [73].

5.3. Cross Linking

Cross-linking is the process that refers to the creation of intermolecular cross-links between bioreceptor molecules and the surface through the formation of covalent bonds. This process involves the use of a multifunctional reagent such as glutaraldehyde or toluene diisocyanate, which binds the bioreceptor molecules together. For instance, glutaraldehyde can crosslink enzyme molecules by reacting with free amino groups of lysine residues of the individual enzyme molecules. The formation of the three-dimensional complex structure or bioreceptor aggregates occurs when this procedure is completed. Immobilization via crosslinking has several advantages, including reduced bioreceptor leakage due to the presence of covalent bonds and the ability to manage the bioreceptor microenvironment to preserve appropriate pH, ionic strength, and other variables. The drawback of this method is that the crosslinking agent might cause changes in the bioreceptor, such as denaturation, which can affect its biological activity at various degrees [74].

5.4. Entrapment

In the entrapment method, a biomolecule, usually an enzyme, is entrapped in a polymeric network that allows the substrate and products to pass through while the enzyme remains trapped. The enzyme is not bound to the support or membrane in this method, unlike the other coupling methods. When cells or cellular organelles are used, entrapment is commonly used. One known method is to passively entrap cells in the pores of membranes made of cellulose or other synthetic materials. Another common method is to use a dialysis membrane to hold the cells or enzymes near the transducer surface. Another option is entrapment in a variety of synthetic or natural polymer gels. Entrapment is one of the simplest immobilization methods because the mediators and additives can be placed in the same sensing layer at the same time [75].

5.5. Affinity Binding

The principle of affinity involves non-covalent interactions based on the establishment of affinity bonds between the activated surface and a particular group of the protein sequence. Complementary biomolecules such as lectin-sugar, antibody-antigen and biotin-avidin have their own natural affinity. This affinity can be exploited in the immobilization technique and leads to remarkable selectivity in detection. The streptavidin-biotin interaction is the best-known technique in this method and results in one of the strongest non-covalent forms. This interaction creates a perfect environment for affinity binding in a variety of fields including immunology, cell and molecular biology. The alternative approach involves the formation of affinity contacts with a protein found only in the Fc regions of an antibody, such as protein A or G [76]. Protein A and G are commonly used for antibody affinity purification and immunoprecipitation. This approach is ideally suited for microarray research as it does not require antibody modification and allows immobilization at high concentrations with good sensitivity [77].

6. ENDOCRINE DISRUPTORS and BISPHENOL A (BPA)

The endocrine system, composed of hormones, controls all biological processes in the body from conception to old age, including brain and nervous system development, reproductive system growth and function, metabolism, and blood sugar levels. In recent decades, there is increasing evidence that a number of substances, also known as endocrine disrupting chemicals (EDCs), may affect the endocrine system and have adverse effects on humans [78]. Polycarbonate by-products, surfactants, insecticides and their metabolites, phthalate plasticizers, polychlorinated biphenyls (PCBs), dioxins, alkyl phenols (APs), bisphenol A, parabens, polycyclic aromatic hydrocarbons (PAHs), etc. are all examples of EDCs that exhibit estrogenic activity. EDCs can affect every system in the body that is controlled by hormones and cause birth defects, cancer and other developmental diseases [79],[80],[81]. Among these EDCs, bisphenol A (BPA) is a highly sought-after chemical that is produced in large quantities worldwide. BPA is used in the manufacture of polycarbonate (PC) and epoxy resins, both of which are ubiquitous in our environment and daily lives. PC is used to make a wide range of food containers and packaging, including drinking bottles, water bottles and cans, tableware, and microwave ovens. Epoxy resins are also used as an interior coating material for painted food cans and bottles [82],[83]. There are a variety of analytical methods for the determination of BPA, including high-performance liquid chromatography, liquid chromatography-mass spectrometry, gas chromatography-mass spectrometry, fluorimetry, chemiluminescence, molecularly imprinted polymers (MIP), and enzyme immunoassay, with chromatography techniques being the most commonly used. These techniques can detect BPA with high sensitivity, but they require skilled personnel, a significant financial investment, and sample preparation and pretreatment, which limits their usefulness [84]. BPA detection methods should be easy to use, take little time, be highly sensitive, and be suitable for real-time detection. Biosensors of various types can be used instead of costly analytical methods [85].

There are many studies in the literature on the detection of BPA using different sensing techniques. Different sensing materials such as molecularly imprinted polymers, carbon nanotubes, graphene, nanocomposites and metal composites are

always used to modify these electrochemical sensors [86]. For example, Maryam et al. have detected bisphenol A in serum samples with a linear range of 0.2-2 nM using an aptamer based on electroactive markers [87]. Liu et al. have developed an electrochemical enzyme biosensor using biochar nanoparticles as signal amplifiers to detect bisphenol A in water [88].

Recently, several types of optical biosensors have attracted much attention to detect EDCs. For instance, Sheng et al. developed an optical biosensor based on fluorescence to detect BPA in water samples, but the response of sensor required the addition of labels [89]. Xue et al. have proposed a novel SPR biosensor that combines a binding inhibition assay with functionalized gold nanoparticles to enable detection of low concentrations of BPA [90]. However, the reaction time of this biosensor is 60 minutes for the detection of BPA, which was too long for rapid detection. Chung et al. have fabricated a surface-enhanced Raman scattering (SERS) based aptasensor platform with double-stranded DNA embedded in Au/Ag nanoparticles with core and shell, which has the highest sensitivity value (10 fM) in a very short time (10 min) for bisphenol A detection [91].

7. USING of ZINC OXIDE (ZnO) in BIOSENSOR APPLICATIONS

Zinc oxide (ZnO) is known as a functional material for many biomedical and biochemical applications due to its nontoxicity, biocompatibility, and strong adsorption ability. ZnO has advanced sensing properties and high isoelectric point (9.5), which enable the detection of biomolecules such as proteins, enzymes, and antibodies. Nanostructured ZnO materials have high active surface area for protein binding and enzyme entrapment by preserving the physiological activity and stability of biomolecules without denaturation compared to their bulk counterparts. For effective signal conversion of biological interactions into physical signals, the biosensor platform requires a specific material with advanced structure, electrical and optical properties. Metal oxides are particularly attractive for biosensor applications as they have all the required physical properties (conductivity, luminescence and absorption) as well as biocompatibility [91]. ZnO known as a metal-oxide semiconductor with a direct wide bandgap (Eg=3.37 eV) has also good chemical-thermal stability, electrical and optical properties. Nanostructured ZnO materials usually used as thin layers have many functions such as attachment of biomolecules, increment of surface to volume ratio, and mechanical protection of the sensing probe in the biosensors [92],[93]. Since ZnO nanostructures are comparable in size to biological molecules, they present prospects for research in biomedical applications, especially biosensors. All these features of ZnO evidence that it is suitable and excellent for transducer applications in various biosensors [94]. ZnO thin films have been fabricated by a variety of methods such as pulsed laser deposition, spray pyrolysis, chemical vapor deposition, RF magnetron sputtering, molecular beam epitaxy (MBE), and sol-gel processing [95].

It is critical to have control over the concentration of intentionally introduced impurities, known as dopants, which are responsible for the electrical and optical properties of ZnO to realize any type of device technology. The dopants determine whether electrons or holes carry the current (and ultimately, the information processed by the device). It is usually possible to achieve one of these types in semiconducting oxides, but not both. Dopants are also known as shallow level impurities because they introduce energy levels that are close to one of the allowed energy bands of material

and are thus easily ionized [96]. Furthermore, the conductivity of the ZnO thin films is increased as a result of doping. Doping of ZnO is accomplished by replacing Zn atoms with atoms of aluminum, potassium, and cobalt [97]. However, doping-induced defects in ZnO are frequently observed, resulting in defects in the fundamental properties of ZnO films. Doping group II elements into ZnO nanostructured oxide films, such as Be, Mg, Ca, Sr, and Ba, change the grain size at the scale and thus the sensitivity of the structure. ZnO is a multifunctional material that can be used in a variety of analytical detection methods, including mass-based biosensors, electrochemical detection, and optical detection. ZnO-based optical biosensors have attracted a lot of interest in healthcare applications because they could significantly improve early diagnostic capabilities with fast response times [15].

Kunene et al. have been used a carbon-screen printed electrode modified with multiwalled carbon nanotubes functionalized with silver doped zinc oxide nanoparticles (Ag-ZnO NPs) on which the laccase enzyme was immobilized to create a novel electrochemical biosensor for the detection of Bisphenol A (BPA) [98]. This proposed biosensor was able to adequately quantify BPA in plastic bottle samples with a highly sensitivity value (6.0 nM). Qiao et al. have fabricated a label-free and novel photoelectrochemical (PEC) aptasensor based on Au nanoparticle modified ZnO as the photoelectric beacon to detect BPA in drinking water and liquid milk samples [99]. Zhang et al. have produced water-soluble Cd doped ZnO quantum dots (QDs) and developed a fluorescence-linked immunoassay (FLISA) method for determining BPA levels in water samples [100]. In this study, the UV–visible and fluorescent analyses showed that QDs are effectively transferred into aqueous solution, and biological mass spectrometry showed that the QDs labeled BPA antibodies successfully. These ZnO based optical biosensors for the detection of BPA are sensitive, rapid, and cost-effective, and thus have great potential in biological and medical applications.

8. SOL-GEL METHOD

In the mid-1800s, Ebelman and Graham published studies on silica gels that received a lot of attention in sol-gel processing of inorganic ceramic and glass materials. According to these early researchers, hydrolysis of tetraethyl orthosilicate $(TEOS)_2Si(OC_2H_5)_4$ under acidic conditions yielded SiO_2 in the form of a "glassy substance" [101]. In 1930, Geffcken found that alkoxides could be used to make oxide films. As shown in an excellent review by Schroeder, this process was subsequently adopted in its entirety and improved by the "Schott glass company" in Germany. Subsequently, mineralogists, ceramicists, and glass scientists used this technology to produce phase diagrams for research, while nuclear physicists used it to produce nuclear fuel. This process was used to produce Ti-SiO_2-TiO_2 reflector coatings in 1959, and metal alkoxide hydrolysis was used to produce SiO_2-B_2O-Al_2O_3-Na_2O-K_2O multicomponent glass in 1971. Sol-gel technology developed rapidly in the 1980s. More recently, it has been used to produce glass, oxide coatings, functional ceramic powders, especially nanooxide materials, functional materials, and composites that are difficult to produce by conventional methods. Fibers, microspheres, thin films, small powders and monoliths can all be produced using sol-gel technology. Protective coatings, catalysts, piezoelectric devices, waveguides, lenses, high-strength ceramics, superconductors, the production of nanoparticles and insulating materials are just some of the other applications of sol-gel technology [102].

The sol-gel method is a wet chemical method of producing vitreous and ceramic materials. In the sol-gel method, a precursor compound with a high chemically active content is used, these raw materials are mixed uniformly in the liquid phase, and chemical hydrolysis and condensation reactions are carried out to produce a stable, clear sol system in solution, which is formed at much lower temperatures than in the usual preparation methods.

It is also used for powderless processing of glasses and ceramics, as well as direct processing of thin films or fibers from solution. The production of thin films is one of the most important applications of sol-gel technology [103]. The sol-gel approach has several advantages over other synthetic methods. The following are some of these advantages:

- The purity and homogeneity properties of the sol-gel product are superior.

- Control of stoichiometry of multiphase systems, particle size, shape and physiochemical properties is possible with sol-gel technique.
- The technique can be used to prepare thin films.
- Sol-gel technique can be used to produce a variety of hybrid materials, both inorganic and organic.
- During the sintering process, the microstructure of the sol-gel process is easier to control (densification process).

Sol-gel technology is used with high efficiency in the fields of electronics, optics, photonics, high temperature technologies, biochemical and biomedical applications due to the above advantages [104].

8.1. Sol-gel Synthesis

In the sol-gel process, hydrolysis and condensation reactions of monomers in a colloidal solution (sol) lead to an integrated network (gel) of nanoparticles or bulky polymerized networks. Metal alkoxides or chloride salts are common precursors for these reactions, but other types of precursors can also be used [105]. Fig. 8.1 shows the schematic view of the sol-gel process that can be summarized, as follows:

- Preparation of the precursor solution.
- Alkoxides are hydrolyzed and partially condensed to form a "sol."
- Polycondensation of hydrolyzed precursors to obtain the gel.
- Aging and drying
- Calcination to obtain materials

The preparation process has a significant effect on the properties of sol-gel materials, such as transparency, porosity, pore size distribution, and surface functionality. The properties of the final material can be fine-tuned by manipulating circumstances during successive stages of the process: Hydrolysis, Condensation, Aging and Drying [106].

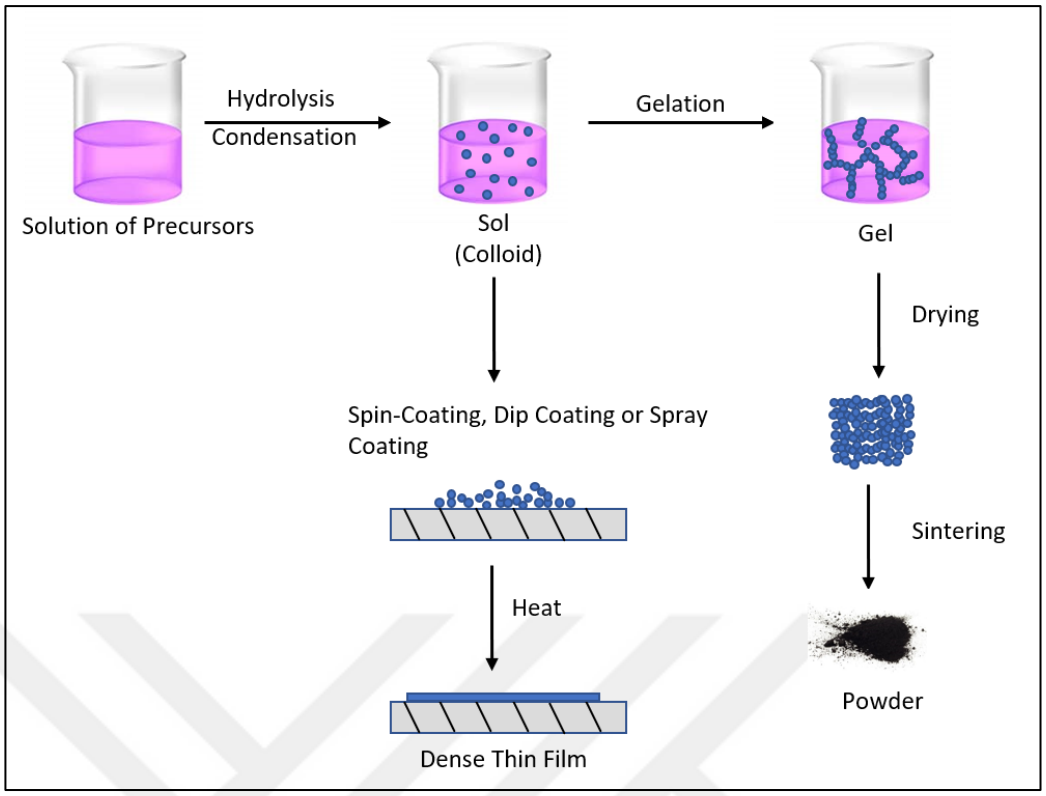

Figure 8.1: A schematic view of sol-gel synthesis

Fig. 8.1 presents a procedure that is neither exhaustive nor limiting. The individual steps can be extended, adapted, or manipulated to meet different requirements, depending on the application. The concentration and type of precursor, the type of solvent, the pH of the solution, the type and concentration of additives (catalysts, surfactants, structuring agents), the pre- and post-heat treatment of the materials and the aging time are all parameters that can be controlled in the sol-gel method [107].

8.1.1. Hydrolysis and Condensation

The reactions listed below explain the hydrolysis, condensation, and polymerization reactions [108].

Hydrolysis:

$$M(OR)_m + nH_2O \rightarrow M(OR)_{m-n}(OH)_n + nROH \quad (8.1)$$

The polycondensation process occurs simultaneously with the hydrolysis

reaction: Partially OH molecules can either react with another OH - containing species under water deprivation (Eq. (8.2)) or react with an alkoxy group to produce an alcohol molecule (Eq. (8.3)).

Condensation of two -OH bearing species:

$$M - OH + HO - M \rightarrow M - O - M + HOH \quad (8.2)$$

Mixed condensation of a -OH group and an alkoxy group bearing species:

$$M - OH + RO - M \rightarrow M - O - M + ROH \quad (8.3)$$

8.1.2. Gelation

The reactions of hydrolysis and polycondensation lead to the formation of clusters that bind together to form a single three-dimensional polymeric network called a gel, the viscosity of which increases rapidly [109]. Gel is a special dispersion system in which colloidal particles or polymers in a sol or solution are connected to each other under certain conditions to form a spatial network structure, and the structural voids are filled with liquid as the dispersion medium (in the case of xerogel, it may also be gas; xerogel is also known as aerogel). The gel is non-flowable and often contains a significant amount of liquid. The percentage of dispersed phase is quite small, ranging from 1% to 3%. Gelation is the term used to describe the process of forming a gel from a solution or sol. In the composition of organisms, gel plays a crucial role. Gels are found in the human body, e.g. in muscles, skin, cell membranes, blood vessel walls, hair, nails and cartilage [102].

8.1.3. Aging, Drying and Calcination

After visible gelation, the sol-gel process proceeds to the aging step, in which the structure and properties of the resulting network continue to change until the desired gel density is achieved. Temperature, pH, solvent and the presence of salts all have a significant influence on the gelation process [110]. Desolvation of the gel transforms the hydro- or alcogel into a porous solid, which is usually accomplished by

solvent evaporation or supercritical drying. To transform the dried gel into a crystalline substance, it is usually calcined. Desorption of solvent and water physically absorbed by the walls of the micropores (100-200°C), decomposition of the remaining organic groups into carbon dioxide (300-500°C), collapse of small pores (400-500°C), collapse of larger pores (700-900°C), and continued polycondensation (100-700°C) are the most common reactions. Sintering and densification are caused by a variety of mechanisms including evaporative condensation, surface diffusion, grain boundary and mass diffusion [111].

8.2. Sol-gel Coating Methods

The variety and simplicity of liquid film deposition processes are made possible for a variety of inorganic and hybrid coating materials by wet chemical sol-gel processes. In general, liquid film deposition involves the application of a liquid precursor film to a substrate, which is then converted to the desired coating material in a post-treatment phase. Dip coating and spin coating are the most commonly used coating processes for industrial and especially laboratory applications due to their ease of use, low cost and good coating quality [112]. External factors such as withdrawal rate, spinning speed, surface tension, viscosity and evaporation rate have a significant influence on the dipping and spinning processes, and the microstructures of the thin films are also affected by these factors [113].

8.2.1. Dip Coating Method

Dip coating is one of the most commonly used coating and thin film processes in the industry. The sol-gel dip coating process requires less equipment and may be less expensive than conventional thin film processes such as chemical vapor deposition, evaporation, or sputtering. The substrate is immersed in the solution during the dip coating process. Dip coating is a batch process in which a thin film is deposited. It can also be performed as a continuous process if the substrate to be coated is a long, flexible sheet or filament. The batch dip coating process involves five stages: dipping, withdrawal, deposition, drainage, and evaporation (see Fig. 8.2). In continuous dip coating immersion is separated from the other steps stages, keeps the withdrawal step

to a minimum, hides drainage in the deposited film and restricts drying to the deposition stage and afterward [114].

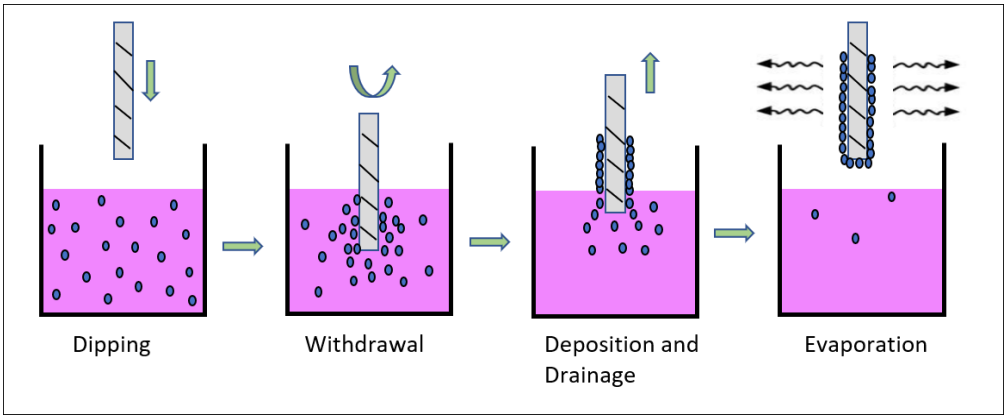

Figure 8.2: Fundamental stages of sol-gel dip coating processes

The ability to control the microstructure of the deposited layer is the greatest advantage of sol-gel over conventional coating processes. When the viscosity of the liquid (η) and substrate speed (U) are high enough in the dip-coating process to reduce the curvature of the meniscus, the ratio of viscous drag ($\alpha\eta$U/h) and gravity force (ρg) is proportional to the thickness of the deposited film (h), as shown in Eq (8.4), where the proportionality constant, c1, is 0.8 for Newtonian liquids, and 0.8 for non-Newtonian liquids.

$$h = c_1(\eta U / \rho g)^{1/2} \tag{8.4}$$

In the case of sol–gel manufacturing, the substrate speed and liquid viscosity are both very low. The ratio of viscous strain to liquid–vapor surface tension (γL, V) calculated from Landau and Levich's relationship controls the balance of substrate speed and liquid viscosity. These were known as the dip coating hydrodynamic factors, which only included pure liquids and ignored temperature. This is expressed in the following equation (8.5):

$$\mathrm{h} = 0.94 \frac{(\eta \mathrm{U})^{2/3}}{\gamma_{\mathrm{LV}}^{1/6} \rho \mathrm{g}^{1/2}} \tag{8.5}$$

The streamline separating the upper and downward moving layers determines

the thickness of the coated films. The thickness and uniformity (streamline) of the deposited film are controlled by six types of forces which act on the film-deposition region.

- The moving substrate creates a viscous pull in an upward direction on the sol.
- The force of gravity
- Gradient in surface tension
- Fictitious Force, also known as inertial force of the boundary coating at deposition zone
- The concave nature of the meniscus causes the inertial force of surface tension to appear
- The pressure of disjoining or conjoining.

The dip coating technique is the link between the study of the structure and properties of the precursor units (sol) and the microstructure of the deposited film. It is one of the oldest and simplest methods of depositing thin films. Although there is no generally applicable model for the dip coating process, the growing knowledge enables the precise fabrication of a wide range of thin film microstructures, from thick films to organized pores.

8.2.2. Spin Coating Method

Spin coating involves forming a layer on a substrate that has been loaded with an inorganic precursor sol and spinning in a controlled manner. Spin coating differs from dip coating in technological terms. This method is basically a batch process which is used evaporation and centrifugal drain delivered by spin for the thinning and deposition of films. The whole method (as shown in Fig. 8.3) can be divided into technical stages [113]:

Deposition: In the deposition stage the sol is loaded onto the substrate and a large amount of sol is applied to the surface of the substrate to coat the entire surface of the substrate.

Spin-up: The substrate which is on the turntable, spins at a controlled speed, and the sol is continually dispensed as the turntable spins. Due to the centrifugal force created by the rotation, the liquid flows radially outward.

Spin-off: Excess liquid flows to the edge of the substrate where it condenses into droplets. The spin-off (the rate at which excess liquid is removed) slows and the film becomes thinner. The thinner film is due to the greater resistance that the solution presents to the flow.

Evaporation: evaporation is the main mechanism of thinning at this stage. This stage usually overlapping and runs concurrently with the spin-off. Drying occurs as a result of evaporation.

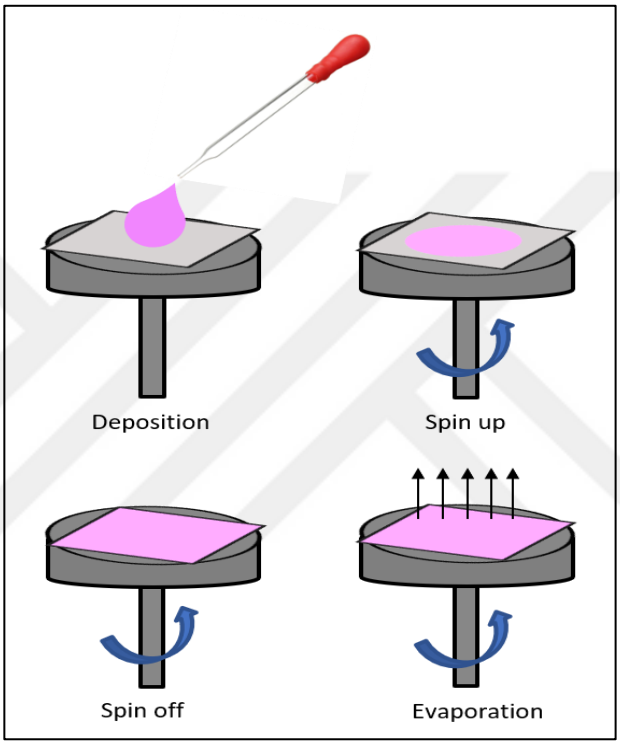

Figure 8.3: Fundamental stages of sol-gel spin coating process

The viscosity of the coating solution and the rotational speed control the thickness of the deposited layer. Eq. (8.6) can be used to calculate the thickness of the deposited film during spin-off:

$$h(t) = \frac{h_0}{(1+4\rho\omega^2 h_0{}^2 t/3\eta)^{1/2}} \tag{8.6}$$

where h0 is the initial thickness of the films, t is the spin time, and is the angular velocity. For the precursor or substrate, ω and ρ are assumed to be constant in ideal conditions.

Spin coating has more advantages over dip coating because the coating

thickness is uniform during the spin-off stage and tends to stay uniform, provided the viscosity does not change across the substrate and is not shear dependent. The balance between the centrifugal force and the viscous force (friction) can explain this tendency. The centrifugal force causes the flow to move radially outward, while the viscous friction causes the flow to move radially inward [115].

9. MATERIALS and METHODS

9.1. Schematic Representation of Ca Doped ZnO Thin Films for Optical Biosensors

In this thesis study, we fabricated porous 10% Ca-doped ZnO thin films (biorecognition layer) using spin coating method (Fig. 9.1. a) to attach biomolecules and amplify optical signals. The aim of this study is to prove the applicability of the thin films we fabricated for optical biosensors. After fabricating the porous thin films, they were functionalized with APTES and GA to immobilize antibodies. The bisphenol A antibody was immobilized on the surface to detect BPA (Fig. 9.1. b). The detection of BPA was done by UV-Vis measurements as shown in Fig.9.1. c-d. Fig. 9.1. shows the schematic representation of the biorecognition layer for the detection of the chemical BPA.

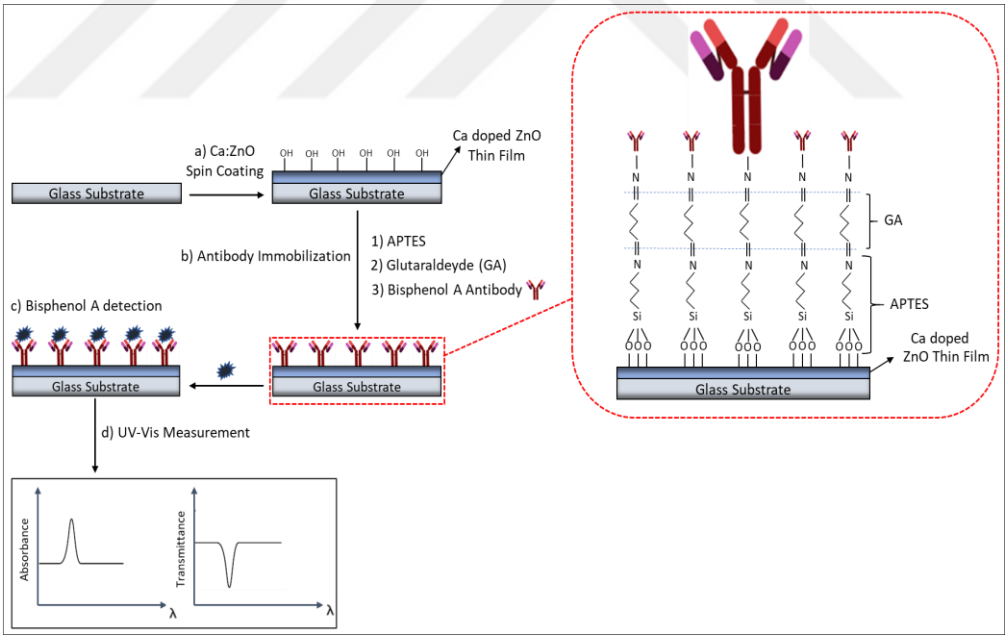

Figure 9.1: Schematic representation of the biorecognition layer for the detection of the chemical BPA. a) 10% Ca-doped ZnO thin film produced by spin coating b) Surface functionalization and antibody immobilization; c) Interaction between antibody and analyte d) Optical measurement (UV-Vis). The right side of the figure shows the magnification of Fig. 9.1 (b) as APTES, GA and antibody immobilization on the Ca-doped ZnO surfaces.

9.2. Cleaning of Substrates

Microscope glass slides, which have less surface defects and good thermal and mechanical resistance, were used as substrates to ensure the quality of the film and the precision of the optical measurements in this study. If these substrates to be coated are not clean enough, it can prevent the formation of a film on the surface and the measurement results can be negatively affected. This is why it is so important to clean glass substrates.

Glass substrates were cut into small pieces (2.5 cm x 2.5 cm) with a diamond pen. Microscopic glass surfaces that have been cut into the desired sizes need to be cleaned of oil and dirt such as dust that is generated when the substrates are cut. Therefore, the substrates were washed with a detergent and cleaned in deionized water, acetone, and ethanol in an ultrasonic bath for 10 minutes each (Fig. 9.2). Before starting the thin film coating, the samples were dried with a heat gun.

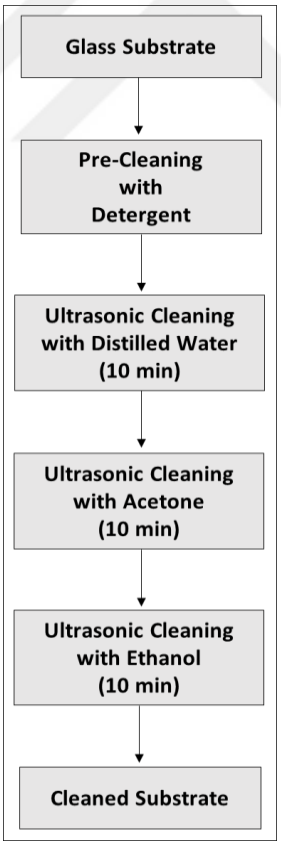

Figure 9.2: Cleaning steps for microscope glass substrates

9.3. Fabrication of Thin Films

9.3.1. Synthesis of Undoped and Ca doped ZnO Solution

Undoped and Ca doped ZnO thin films were synthesized on glass substrates by sol-gel dip coating and spin coating method. Zinc acetate dihydrate ($Zn(CH_3COO)_2$-$2H_2O$), ethanol (C_2H_5OH), diethanolamine ($C_4H_{11}NO_2$, DEA) and deionized water (H_2O) were used as precursor, solvent, sol stabilizer and catalyst, respectively. Calcium acetate hydrate ($Ca(CH_3COO)_2$) was used as Ca doping source. The properties of the chemicals used are listed in Table 9.1.

Table 9.1 Chemical formula of substances for Thin Films

Chemical Substance	**Chemical Formula**	**Molecular Weight (g/mol)**	**Purity (%)**
Zinc Acetate Dihydrate	$Zn(CH_3COO)_2 \cdot 2H_2O$	219.5	99.0 - 101.0%
Calcium Acetate Hydrate	$Ca(CH_3COO)_2$	158.17	93.0-95.0%
Diethanolamine	$C_4H_{11}NO_2$	105.14	99%
Ethanol	C_2H_5OH	46.07	≥99.9%
Deionized Water	H_2O	18.02	99.9%

In the undoped synthesis, 4.39 g of zinc acetate dehydrate was first dissolved in 34.49 ml of ethanol and then 1.91 ml of DEA was added to the solution. The concentration of zinc acetate was 0.5 M and the molar ratio of DEA to zinc acetate was kept at 1:1. The precursor solution was stirred with a magnetic stirrer on a hot plate at 60℃ for 1 hour until a homogeneous and transparent solution was obtained. After adding 1.08 ml of water dropwise to the solution and stirring again for 1 hour, the temperature was lowered to 25℃. The molar ratio of water to zinc acetate was 3:1. Aging time of solutions is different, and solution aging times are 5 days and 1 day for dip coating and spin coating methods, respectively.

For Ca-doped ZnO thin films, different Ca concentrations were added to the sol solutions by dip and spin coating. Calcium acetate hydrate was added to the ZnO

solution at a concentration of 1% and 5% of the dopant immediately before the addition of water. The solution was used to coat the glass substrate by dip coating method. Based on the experimental results, it was found that the Ca concentration in the sol solution should be increased. Therefore, the Ca concentration was increased to 10% in the spin coating method. Additionally, PEG 400 known as surfactant was added at different concentrations to Ca doped ZnO thin films to examine the effect on the volume of surface porosity. ZnO-to-PEG ratios of 3:0.5 and 3:1 was investigated in these thin films produced by spin coating method.

The schematic flow diagram for the synthesis of the undoped and Ca doped solutions is summarized in Fig. 9.3.

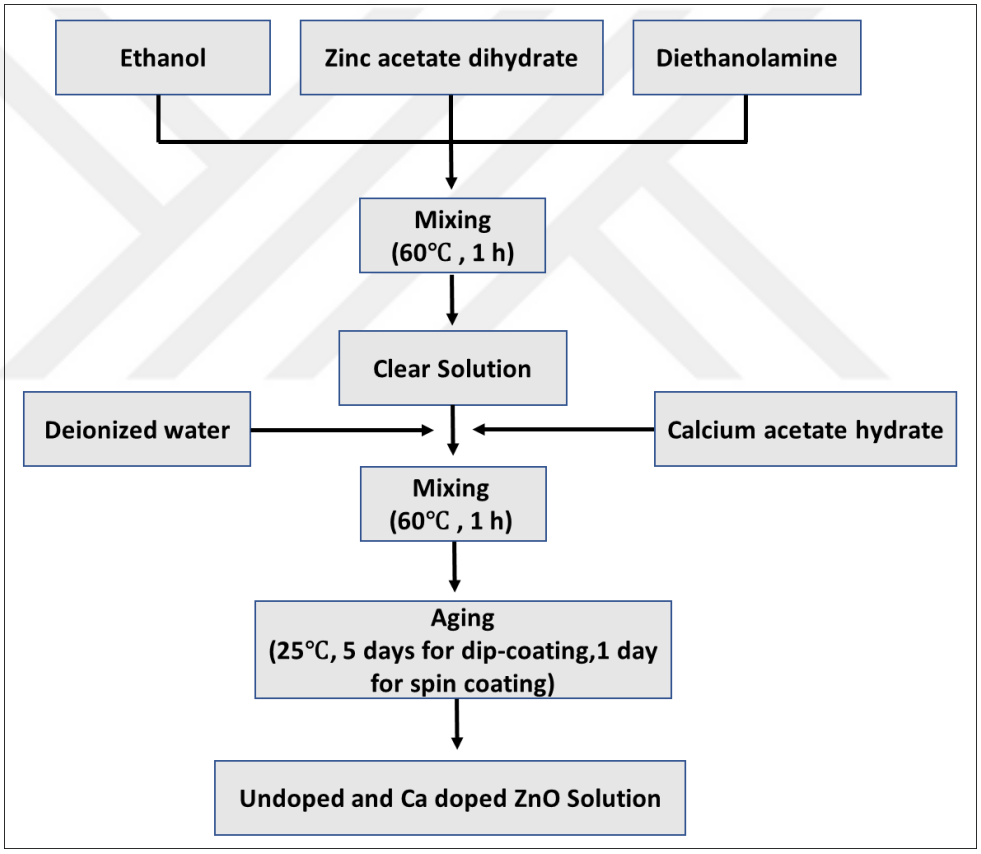

Figure 9.3: Flowchart of undoped and Ca doped ZnO solution

9.3.2. Fabrication of Undoped and Ca doped ZnO Thin Films with Dip-Coating Technique

The solution was deposited on glass substrates by dip- coating at a withdrawal speed of 100 mm/min. After each coating, the drying process was carried out at 300℃ for 60s to completely evaporate the organic components and the residual solvent. The dipping process was repeated 10 times for each sample. Finally, the resulting thin films were heat treated at 500℃ for 1 hour to ensure that all organic components organics were expelled from the films. The thin films were fabricated according to the flow chart shown in Fig. 9.4.

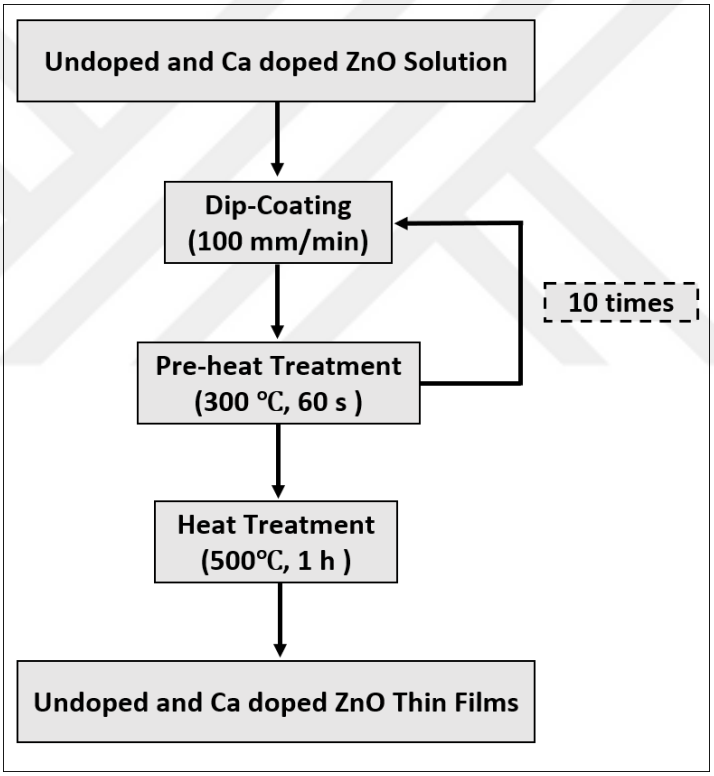

Figure 9.4: Flowchart of undoped and Ca doped ZnO thin films with dip-coating method

9.3.3. Fabrication of Undoped and Ca doped ZnO Thin Films with Spin Coating Technique

The deposition was carried out in air in three steps at different spin speeds, namely 2000 rpm for 30 s, 3000 rpm for 40 s and 4000 rpm for 50 s. After each coating,

the films were preheated at 300℃ for 5 min on a hot plate. This coating procedure was repeated 15 times. After deposition of the last layer, the resulting films were postheated in air at 500℃ for 1 hour. The flow chart of the spin coating steps to form a thin film is shown in Fig. 9.5.

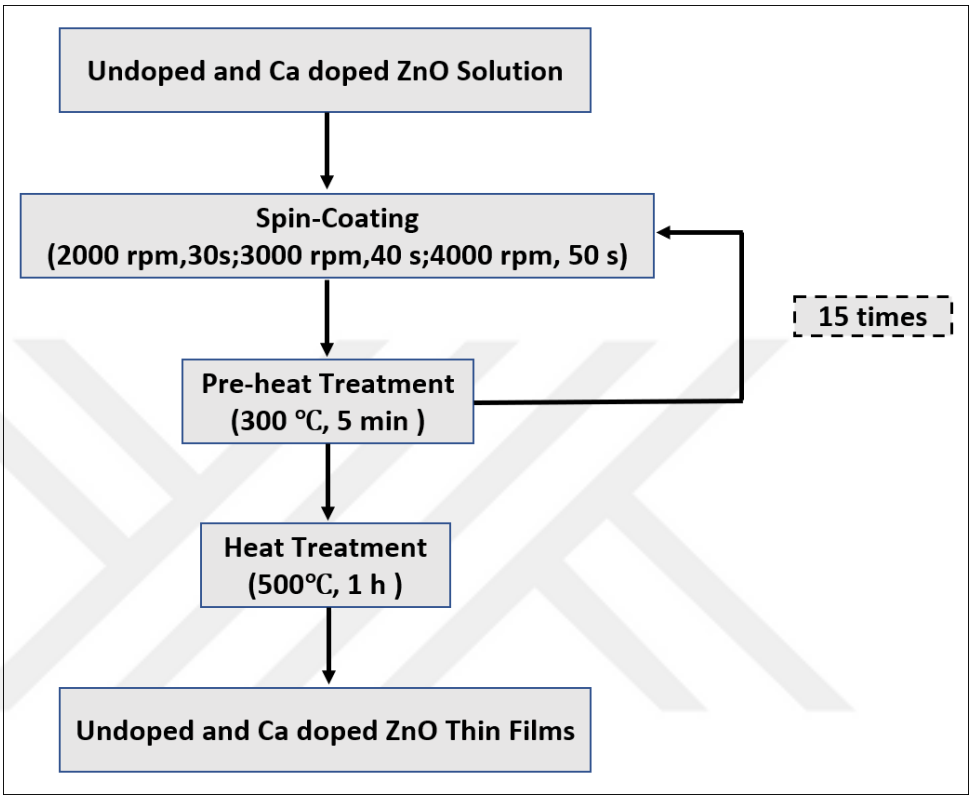

Figure 9.5: Flowchart of undoped and Ca doped ZnO thin films with spin coating method

9.3.4. Surface Functionalization of 10% Ca doped ZnO Thin Films

Surface functionalization was carried out on the surface of the 10% Ca doped ZnO thin films by using silane chemistry. The chemical substances used for this process are listed in Table 9.2. Condensation reactions can take place between the amine groups of the APTES and the hydroxyl groups of the Ca doped ZnO surface [116]. Fig. 9.1. shows the functionalization steps, which include modification with 3-aminopropyltriethoxysilane (APTES), glutaraldehyde (GA), antibody binding, and analyte binding (bisphenol A). Surface functionalization with APTES has been shown in the literature to increase surface adhesion, improve film quality, and immobilize biomolecules on biorecognition layers for biosensors [117]. First, the thin films were

immersed in a 2% solution of APTES in DI water for 1 hour. After APTES functionalization, the thin films were washed with DI water and dried with nitrogen gas. Then, the thin films were immersed in a 2.5% GA with DI water for 30 min to introduce the aldehyde group on the amine-terminated surface of thin films. The functionalized thin films were washed with deionized water and dried with nitrogen gas just before the antibody was immobilized.

Table 9.2 Chemical substances used in Functionalization Process

Chemical Substance	Chemical Formula	Molecular Weight (g/mol)
3-aminopropyl triethoxysilane (APTES)	$C_9H_{23}NO_3Si$	221.37
Glutaraldehyde (GA)	$C_5H_8O_2$	100.11

9.3.5. Antibody Immobilization on the Functionalized Thin Films

Polyclonal bisphenol A antibodies were purchased from Fitzgerald (North Acton, MA, USA). We prepared solution at dilution rate (1:10.000) for binding of the antibodies to the surface. The functionalized thin films were immersed 1µl of antibody in 10 mL phosphate buffer solution (PBS) (pH 7.4) for 1 h at 4 °C to allow the antibody molecules to react with aldehyde groups and bind to the surface of the Ca doped ZnO thin films. Finally, the thin films were washed three times with PBS to remove excess molecules.

9.3.6. Different concentrations of the chemical Bisphenol A as an Analyte

Bisphenol A (BPA; 2,2-bis-(4-hydroxyphenyl) propane) was purchased from Sigma-Aldrich. Working solutions of analyte (BPA) were prepared from stock solution by dissolving 40 mg of BPA in 40 ml of a mixed solution of methanol and PBS (1:1). Different working solutions were prepared with concentrations of 50, 100, 200, and 300 ng/mL. The antibody-immobilized thin films were placed in these BPA solutions for 1 hour to detect the chemical BPA.

9.4. Thermogravimetry/Differential Thermal Analysis (TG/DTA)

Netzsch STA 449 F3 Jupiter thermal analysis was used to measure of mass changes and thermal effects with a heating rate of 0.5°/min from 20°C and 600°C.

9.5. X-ray Diffraction (XRD) Analysis

The crystal structure of ZnO thin films and ZnO powder samples were analyzed using X-ray diffraction (XRD-Rigaku Dmax 2200) with Cukα radiation (λ = 1.5405 Å) at a rate of 0.5°/min in the range of 20-60°.

9.6. Scanning Electron Microscopy (SEM) Analysis

Both the surface and cross-sectional areas of the produced thin films were examined using a Phillips XL 30 SFEG Scanning Electron Microscope. The surface morphology of thin films is an important tool for studying their microstructure. The prepared films are coated with a very thin layer of gold by sputtering before imaging to increase conductivity. While the surface images were used to investigate whether there are micro/nano cracks, pores or crystallizations, the cross-sectional image was used to determine the film thickness.

9.7. Phyton Analysis of Thin Films

Image processing libraries in Python were used to calculate surface porosity in SEM images using image analysis software (version 3.9.1). The captured images using SEM which was taken to calculate the surface porosity are in RGB color space and each image saved as ".tif" file. The pore analysis of each image with a size of 712 × 425 pixels was done with this data analysis method. The porosity of ZnO thin films was determined using the image volume method after SEM converted images of ZnO thin films into binary images. This method measures the volume of porosity on the entire image area. The volume porosity is calculated by adding the area of the porosity

pixels and dividing by the total area of the images. Then the result is multiplied by 100%.

9.8. Atomic Force Microscopy (AFM) Analysis

The Nanoscope spectrophotometer IV AFM was used in contact mode to measure the three-dimensional surface images and surface roughness of Ca doped ZnO thin films and APTES-GA functionalized Ca doped ZnO thin films, respectively. Each sample scan was made over each 1 cm × 1 cm sample.

9.9. Prism Coupler Analysis

Measurements of the refractive index of thin films were made using the Metricon model 2010/M prism coupler. The prism coupler is a device that allows high-precision measurement of parameters such as the refractive index and thickness of a light-guiding thin film.

9.10. UV-Vis-NIR Spectrophotometer Analysis

The UV-3600i Plus model UV-Vis-NIR spectrophotometer was used to study the optical properties of the thin films. The optical properties of the undoped and 10% Ca-doped ZnO films, APTES-GA functionalized thin films, and antibody-immobilized thin films were investigated using the UV-Vis NIR spectrophotometer in the wavelength range of 300-800 nm. The absorption and transmission spectra were recorded for all measurements. In addition, the UV-Vis-NIR spectrophotometer was used as an optical transducer for the detection of BPA.

10. RESULTS AND DISCUSSION

The "Results and Discussion" section is divided into four sections: dip coating results, spin coating results, functionalization and immobilization of thin films, and BPA detection.

10.1. Microstructure, Phase and Optical Analysis of Thin Films Produced by Sol-Gel Dip Coating Method

10.1.1. TG/DTA Results of ZnO Thin films

Fig. 10.1 shows the TG/DTA curves of undoped ZnO. In the TGA plots, two endothermic peaks were observed in the DTA curve at 100 °C and 260 °C, which were associated with a large weight loss. These peaks were probably caused by the evaporation of water and the decomposition of zinc acetate. Weight loss due to organic residue removal was also associated with an exothermic peak at 484.80 °C. Therefore, a sintering temperature of 500 °C was chosen, which was above the temperature range of the weight loss.

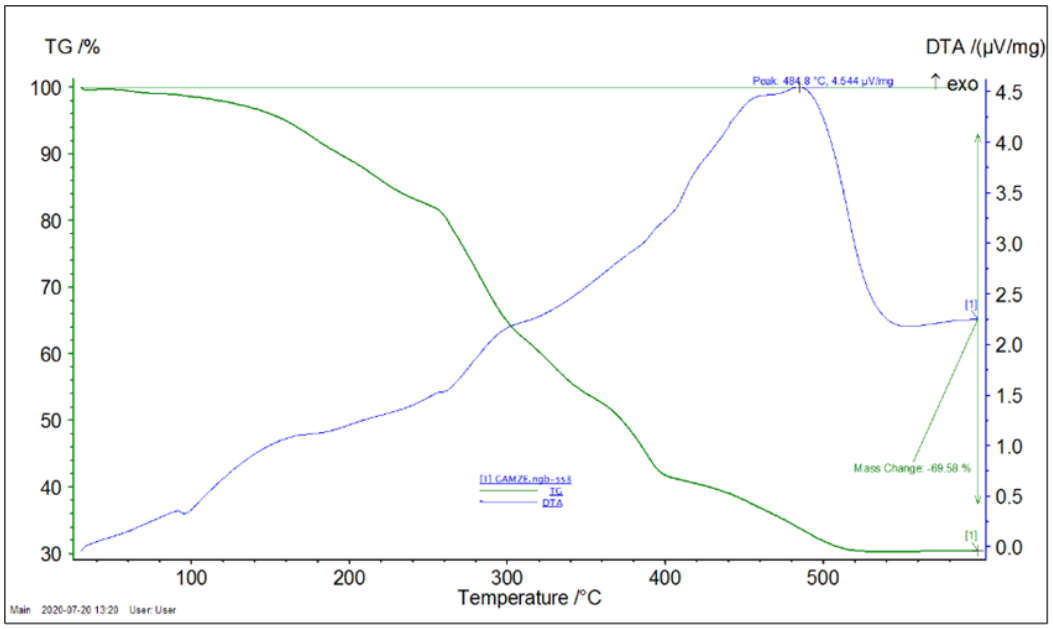

Figure 10.1: TG/DTA curves of dried gel obtained from undoped ZnO solution

10.1.2. XRD Analysis of ZnO Powder Sample

X-ray diffraction (XRD) method was used to characterize the undoped ZnO powder as shown in Fig.10.2. The examination revealed a polycrystalline wurtzite hexagonal ZnO structure (JCPDS 89-0510). There was a slight orientation along the (101) axis. The XRD peaks of 31.78°, 34.43°, 36.26°, 47.55°, 56.61°, 62.87° and 67.96° corresponded to the orientations of ZnO (100), (002), (101), (102), (110), (103) and (112), respectively.

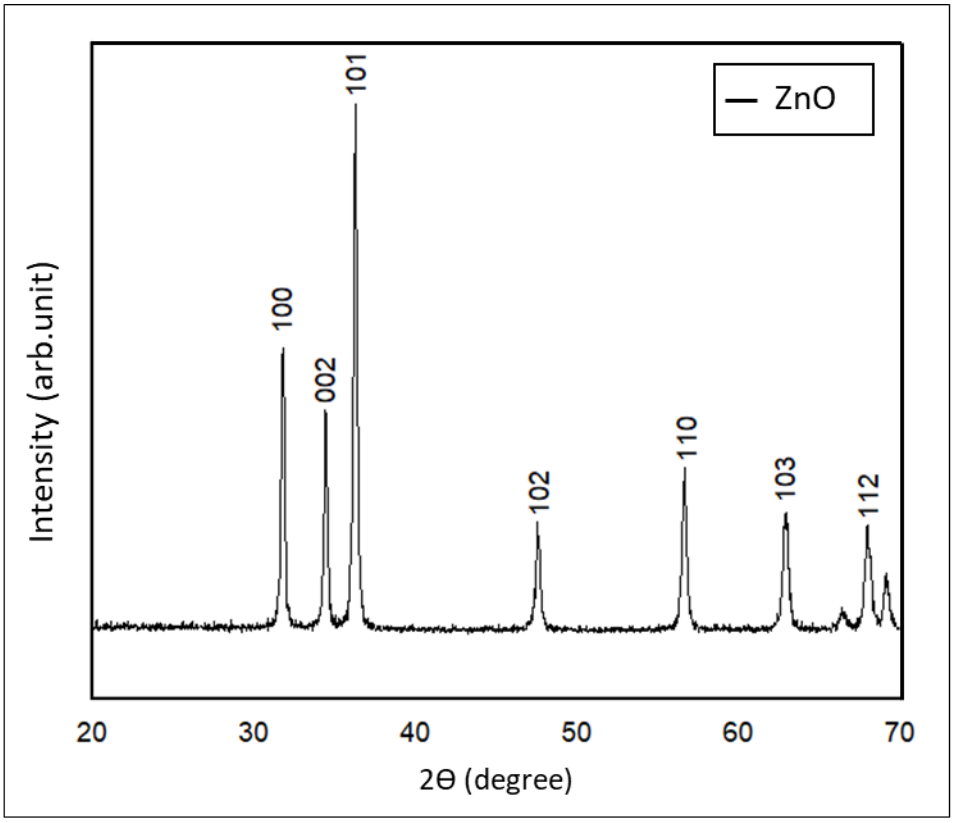

Figure 10.2: XRD pattern of undoped ZnO dried powder

10.1.3. SEM Analysis of Thin Films

Fig.10.3(a-c) shows SEM micrographs of Ca doped ZnO thin films (0%, 1%, %5) respectively as undoped, 1% and 5% at low and high magnifications. Formed a structure of ZnO nanorods in the ZnO films can be demonstrated by the SEM observations. Additionally, on the top of the surface, equiaxed grains were also observed. Fig. 10.4 shows a cross-sectional sketch of ZnO nanorods with equiaxed

grains at the top of the surface [125]. Although ZnO thin films often form a preferred orientation in the (002) direction, equiaxed grains at the top of the thin films have no such preference. Moreover, 1% Ca doped ZnO thin films were found to decrease the diameter of the nanorods, as shown in Fig.10.3 (b). However, increasing the Ca doped ZnO content to 5% has no effect on the diameter of the structure (see Fig.10.3 (c)).

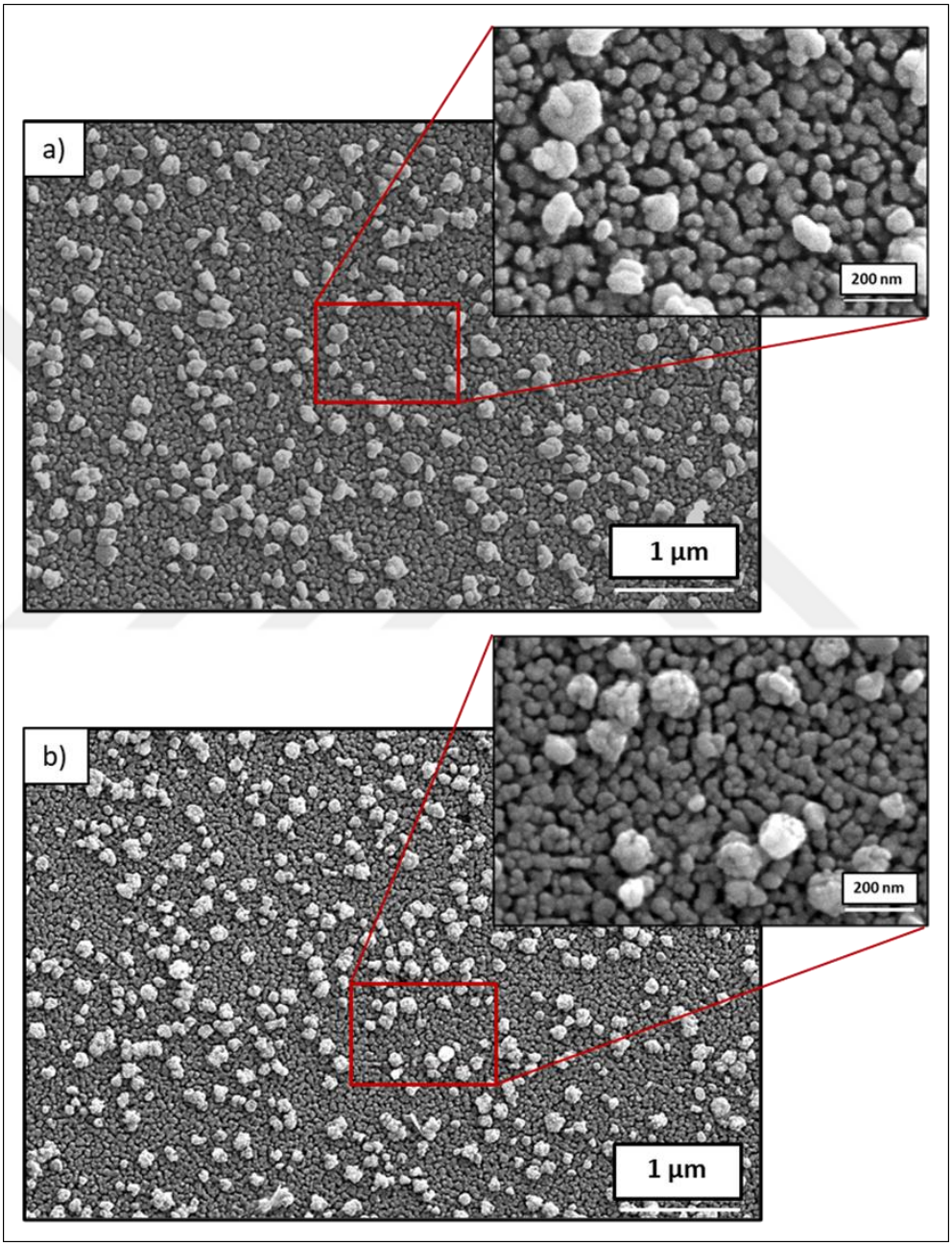

Figure 10.3: SEM micrographs of undoped and Ca doped ZnO thin films with dip-coating method: a) ZnO b) 1%-Ca:ZnO c) 5%-Ca:ZnO

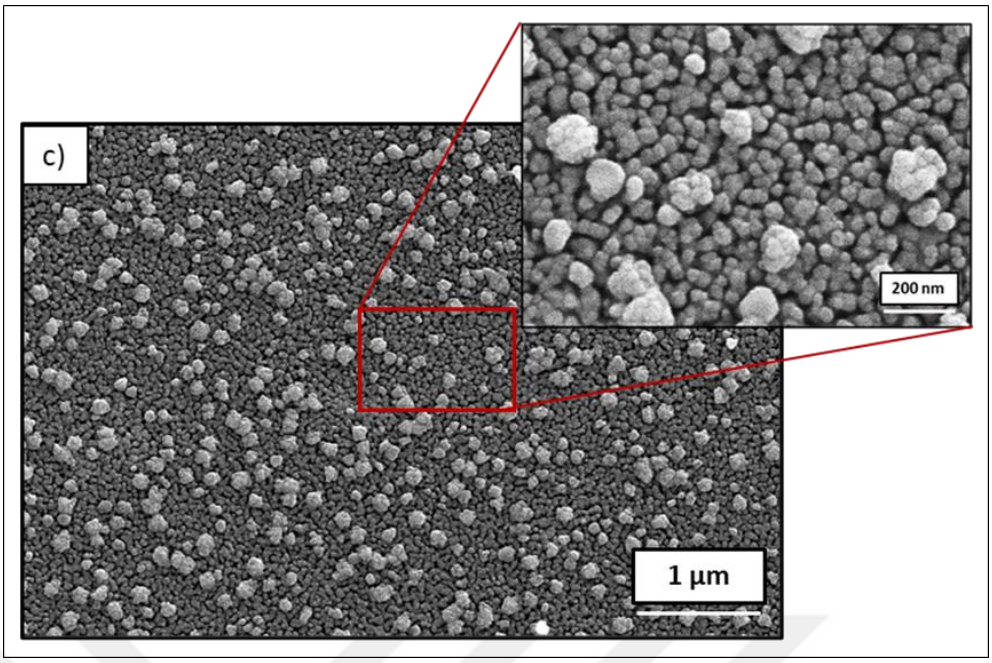

Figure 10.3: Continued

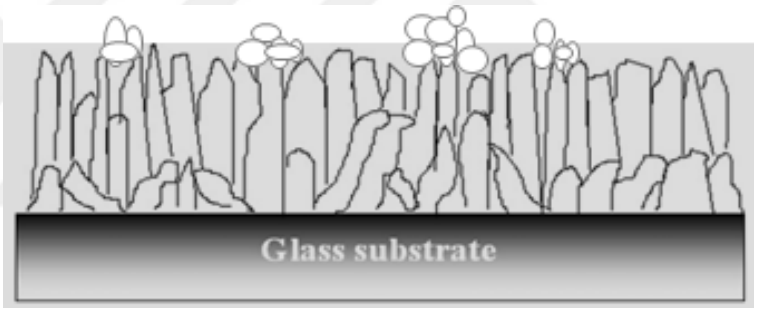

Figure 10.4: Description of a basis orientation of ZnO thin films (not drawn to scale) with white grains on the top of the surface [125].

10.1.4. Python Analysis of Thin Films

The volume porosity values were determined Python image processing as 9.08%, 14.24%, and 12.12% for undoped ZnO, 1%-Ca:ZnO, and 5%-Ca:ZnO, respectively. Ca doping at these concentrations has not significant effect on the surface porosity of the ZnO thin film (Fig. 10.5).

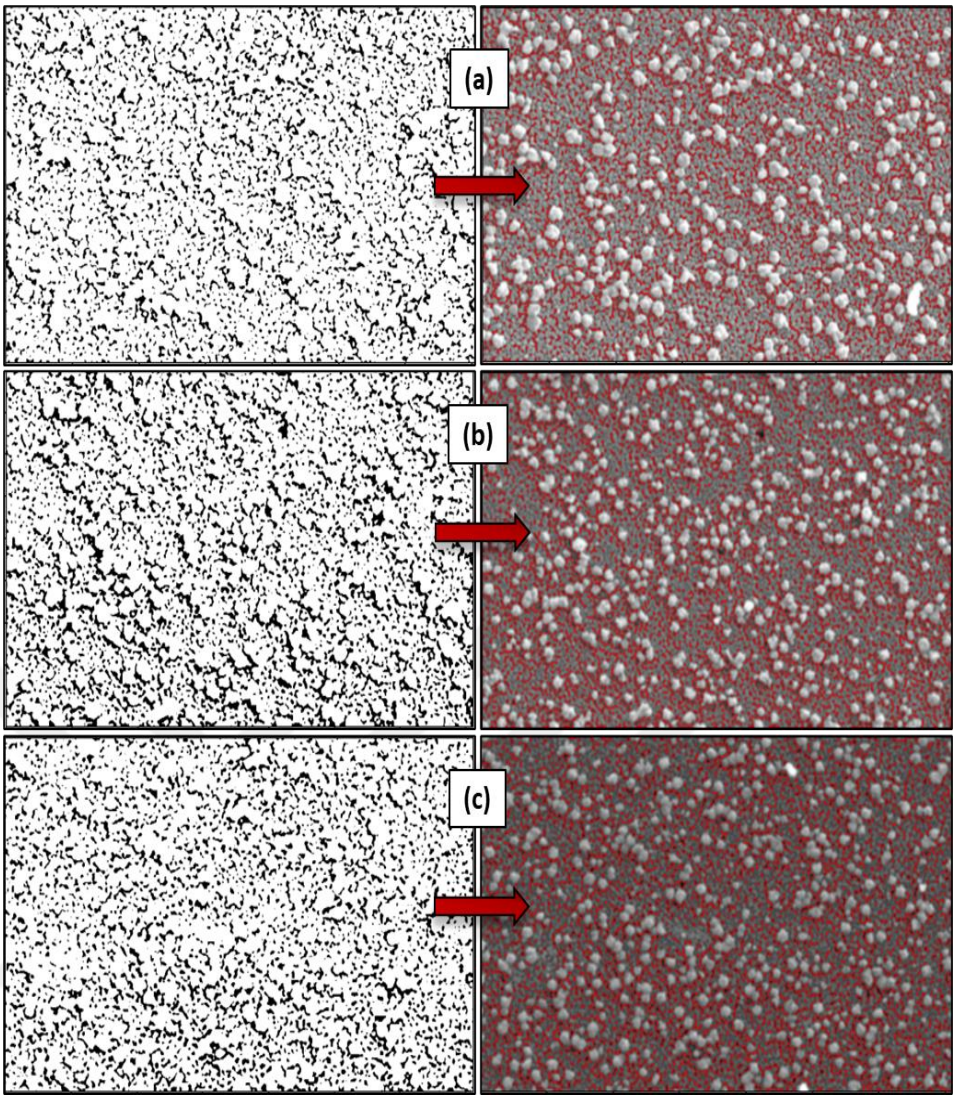

Figure 10.5: Binary images of SEM micrographs made by image processing libraries in Python as: a) undoped ZnO b) 1%- Ca:ZnO c) 5%-Ca:ZnO

10.1.5. Prism Coupler Measurements of Thin Films

The Metricon 2010 Prism Coupler was used to measure the refractive index values of films. The weighted average of the refractive indices of CaO (1.84) and ZnO (2.00) was used to calculate the theoretical refractive index of 0%, 1%, and 5% Ca doped ZnO thin films. Three different points of each film were used to obtain the measured mean refractive index values. The results of the refractive index measurements and the calculated percentage of porosity of the films are shown in Table 10.1. Compared to 1% Ca doping, the refractive index of 5% Ca doping increased with decreasing porosity. Istrate et al. found similar results with 5% Ca

doped ZnO at a concentration of 0.5M [15]. The increased film density and improved crystallinity in 5% Ca doped ZnO thin films resulted in a higher refractive index, according to these researchers. Ca doped ZnO thin films exhibit higher porosity than undoped (0%) ZnO thin films, as measured by refractive index and calculated with Python from SEM images.

Table 10.1 The measurement refractive index and % porosity of Ca doped ZnO thin films.

% Ca doping	**Theoretical refractive index**	**Measurement refractive index**	**% porosity (calculated by refractive index values)**	**% porosity (calculated by Python from SEM images)**
0	2.000	1.9914 ± 0.02	1.13	9.08
1	1.9985	1.9671 ± 0.01	4.16	14.24
5	1.9924	1.9786 ± 0.01	1.84	12.12

We did not observe a sufficient effect on surface porosity at the 1% and 5% Ca concentrations. Moreover, we increased the Ca concentration to 10%, but a homogeneous coating could not be achieved by the sol-gel dip coating method. Therefore, we proceeded with the spin coating method to produce 10% Ca doped ZnO thin films.

10.2. Microstructure, Phase and Optical Analysis of Thin Films produced by Sol-Gel Spin Coating Method

10.2.1. XRD Analysis of Powder Samples

The XRD patterns of the undoped ZnO, 10% Ca doped, PEG added (3:0.5 and 3:1 ZnO: PEG) 10% Ca doped ZnO powder samples are shown in Fig. 10.6. The XRD peaks of 31.7°, 34.42°, 36.25°, 47.53° and 56.60° correspond to ZnO orientations (100), (002), (101), (102) and (110), respectively. Compared to the ZnO thin films, an additional peak (as shown in Fig. 10.6) at 2θ of 29.4° was detected in all Ca-doped

ZnO powder samples. It corresponds to the strongest signal of the calcite ($CaCO_3$) phase [118]. This indicates that calcium does not disperse completely as an isolated impurity, but is preferentially segregates into calcite, which has the same hexagonal unit cell structure as wurtzite.

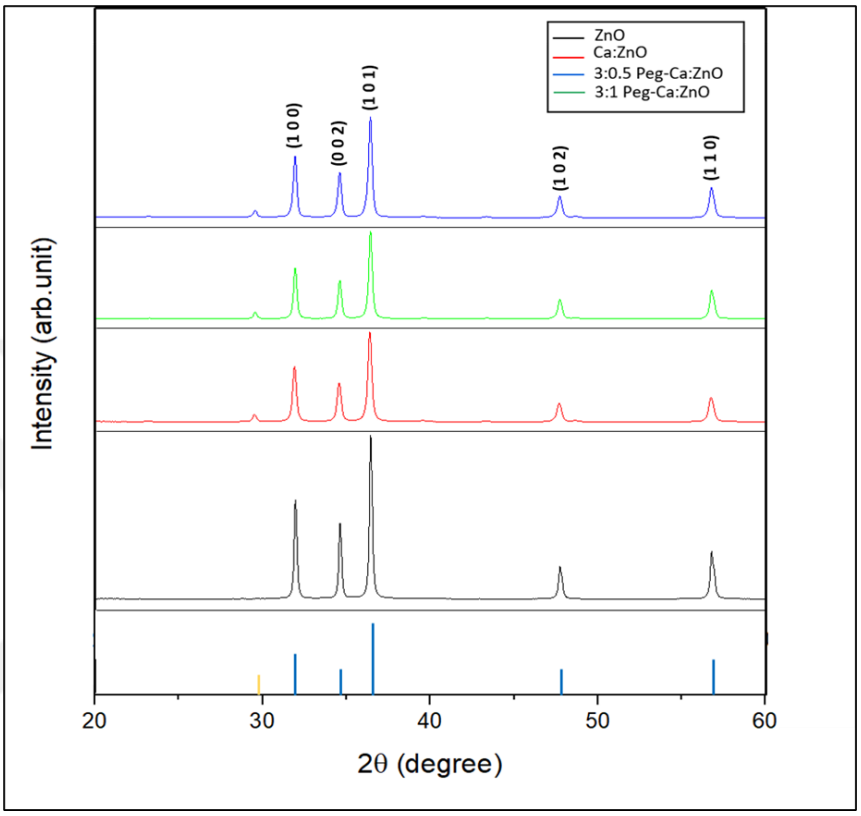

Figure 10.6: XRD pattern of dried undoped and 10% Ca doped ZnO powder samples

The crystallite sizes of undoped and Ca doped ZnO thin films were calculated by Scherer's formula:

$$D = \frac{k\lambda}{\beta\cos\theta} \qquad (10.1)$$

where $\boldsymbol{\lambda}$ = 0.154 nm is the wavelength of the X-ray radiation used, $\boldsymbol{\theta}$ is the Bragg diffraction angle of the XRD peak and $\boldsymbol{\beta}$ is the full width at half maximum (FWHM) of the diffraction peak. Ca doping causes an increase in the value of FWHM of (1 0 1) peak and an decrease in the crystallite size. The crsytallite size of the ZnO in the films prepared by spin coating method decreases from 34.90 nm (ZnO) to 26.15 nm (Ca doped ZnO).

10.2.2. XRD Analysis of Thin Films

Fig. 10.7 shows the XRD patterns of undoped and Ca doped ZnO thin films deposited by the spin coating technique at room temperature. From the XRD analysis, both the undoped ZnO film and the Ca doped ZnO thin films exhibit polycrystalline films with wurtzite hexagonal structure of ZnO (zincite) (JCPDS card no. 36-1451). The XRD peaks of 31.7°, 34.42°, 36.25°, 47.53° and 56.60° correspond to the orientations of ZnO (100), (002), (101), (102) and (110), respectively. All the studied samples exhibited preferential orientation in the (101) atomic plane. The hexagonal wurtzite symmetry was maintained with Ca concentration. Furthermore, the addition of PEG to thin films caused a decrease in the (002) peak in the ZnO lattice and no calcite phase was observed at a 2θ of 29.4° in the thin films.

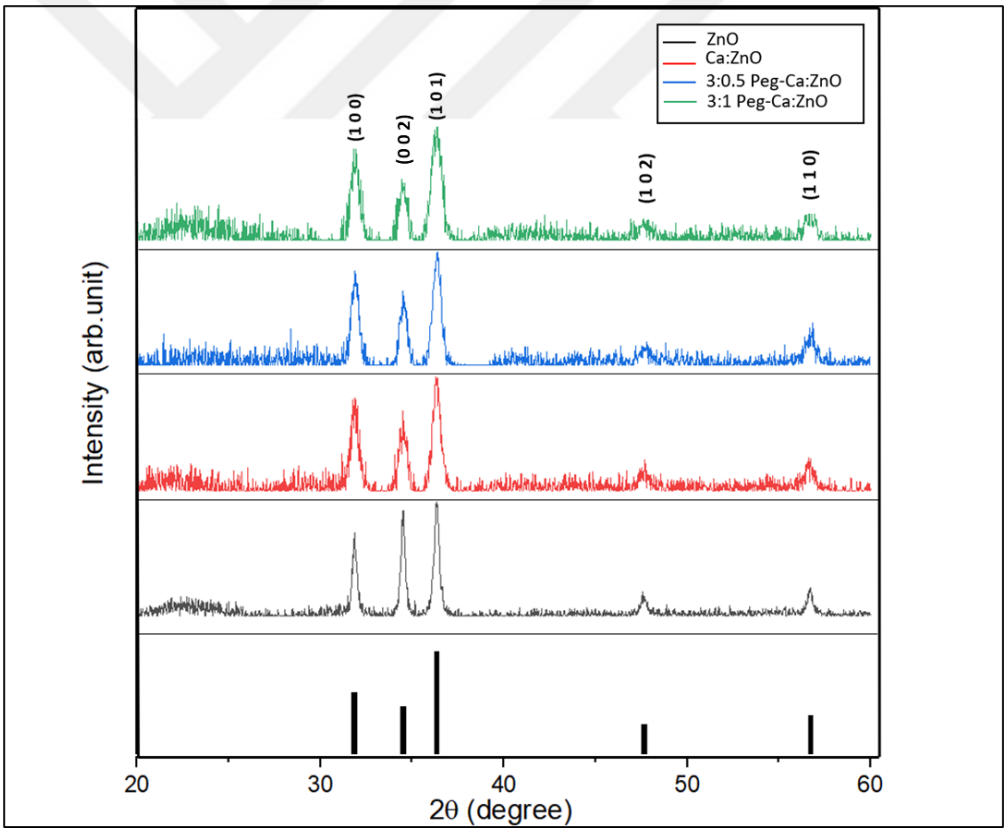

Figure 10.7: XRD pattern of undoped and 10% Ca doped thin films

10.2.3. SEM Analysis of Thin Films

The surface morphology of 10% Ca doped ZnO thin films with/without 3:0.5 and 3:1 ZnO: PEG doping is shown in Fig. 10.8(a-d). The undoped ZnO thin films, the 10% Ca doped ZnO thin films and the PEG added 10% Ca-doped ZnO thin films were deposited on glass substrates by sol-gel spin coating method.

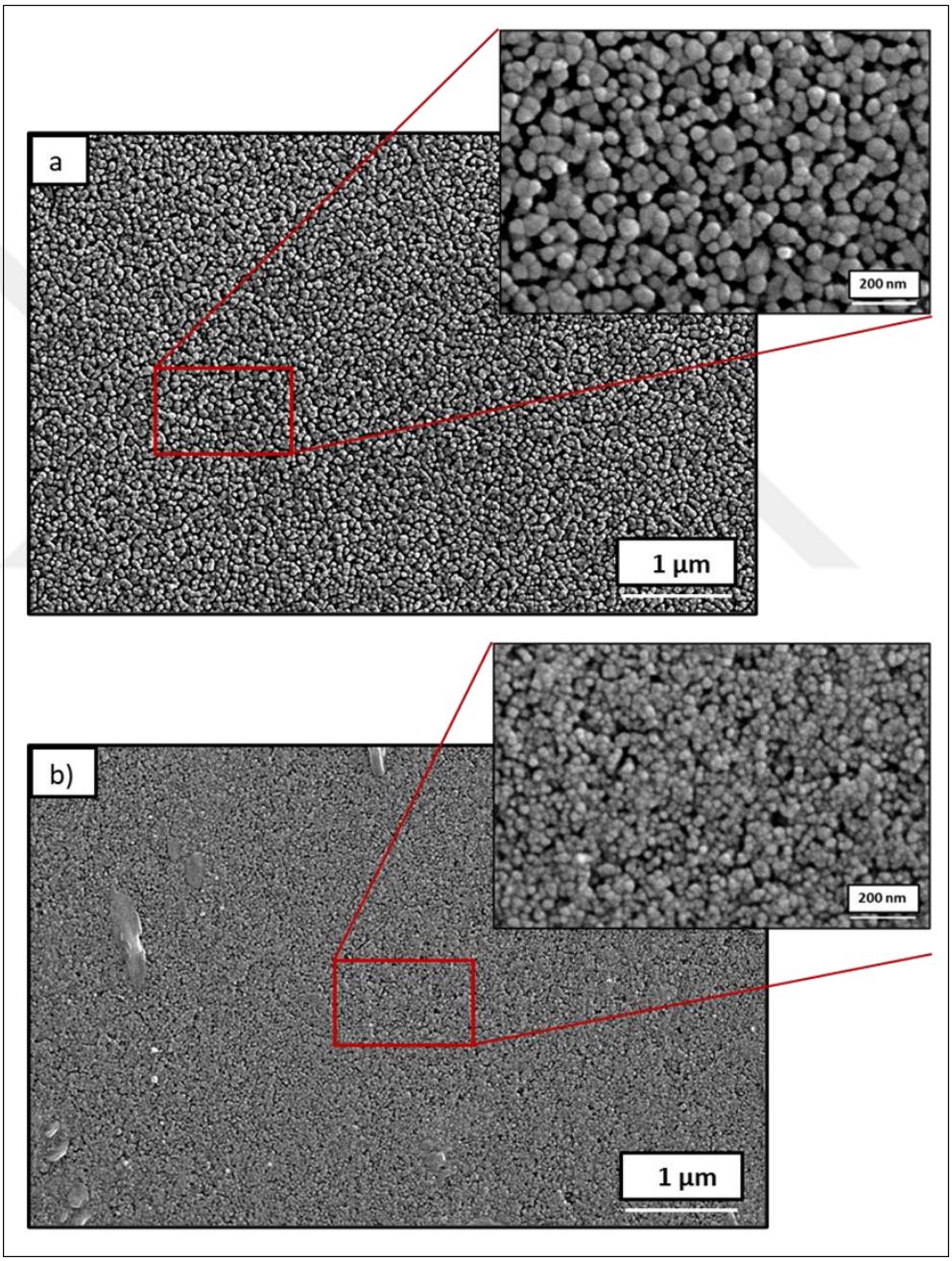

Figure 10.8: SEM micrographs of undoped and 10% Ca doped ZnO thin films with spin coating method: a) undoped ZnO b) 10% Ca doped ZnO c) 3:0.5 PEG-10% Ca:ZnO d) 3:1 PEG-10% Ca:ZnO

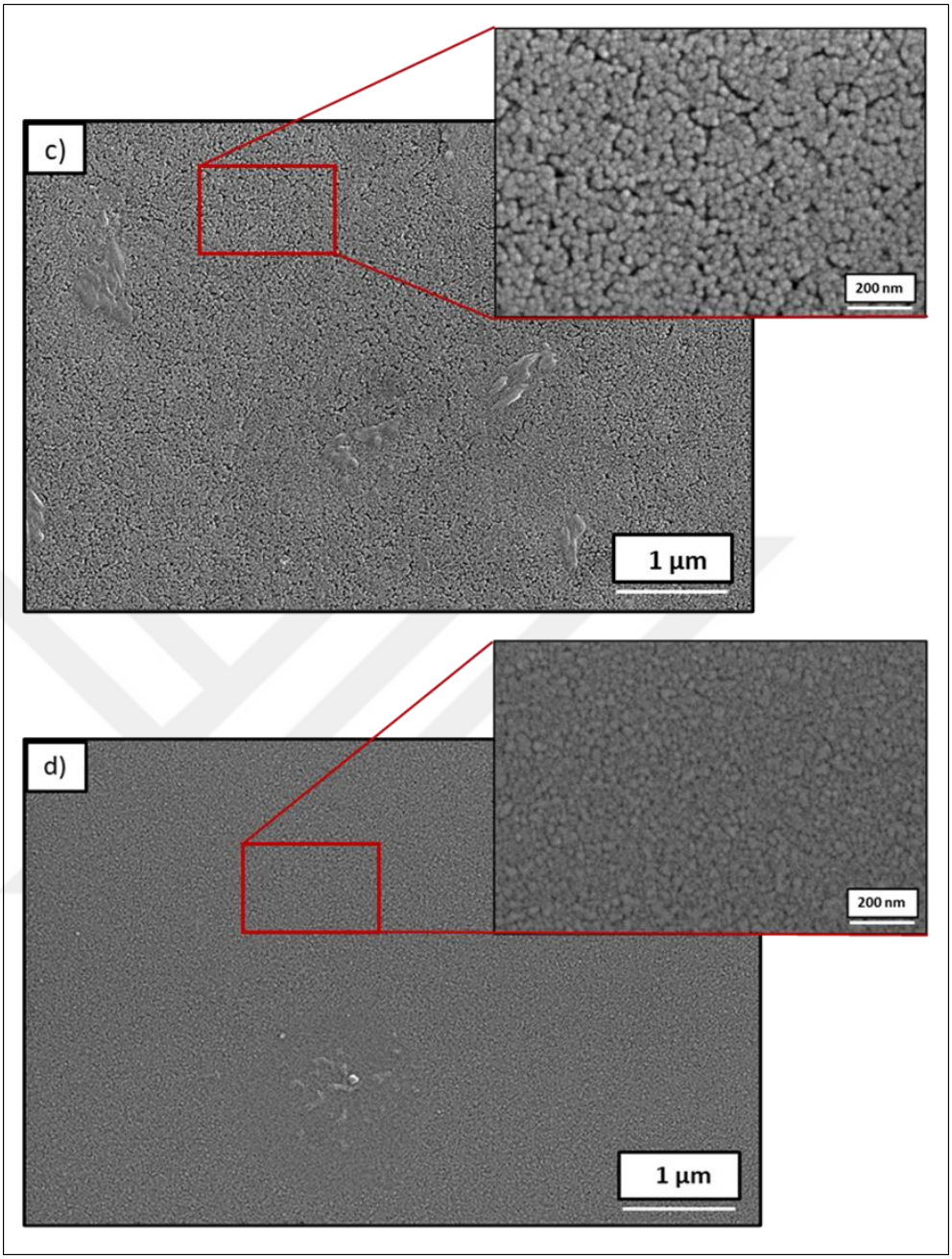

Figure 10.8: Continued

Fig. 10.8 (a and b) clearly shows the highly porous structure of the undoped and the 10% Ca doped ZnO thin films. It can be seen that the undoped and 10% Ca doped films are porous without PEG, as shown in Fig.10.8 (a and b), and with the addition of PEG to 10% Ca doped ZnO thin films, the microstructure was found to be uniform with compact connected grains. Moreover, the porosity gradually disappeared when the PEG content was increased, as shown in Fig.10.8 (c and d). Fig. 10.8 (b) shows that 10% Ca doping leads to a decrease in crystal and pore size compared to

undoped ZnO films (Fig. 10.8 (a)). These nm-sized pores lead to a larger surface area in Ca-doped ZnO thin films than in undoped ZnO thin films. Therefore, the number of bioreceptor attachments can be increased by using Ca-doped ZnO thin films in the development of our biosensor. This will directly affect the sensitivity of the biosensor.

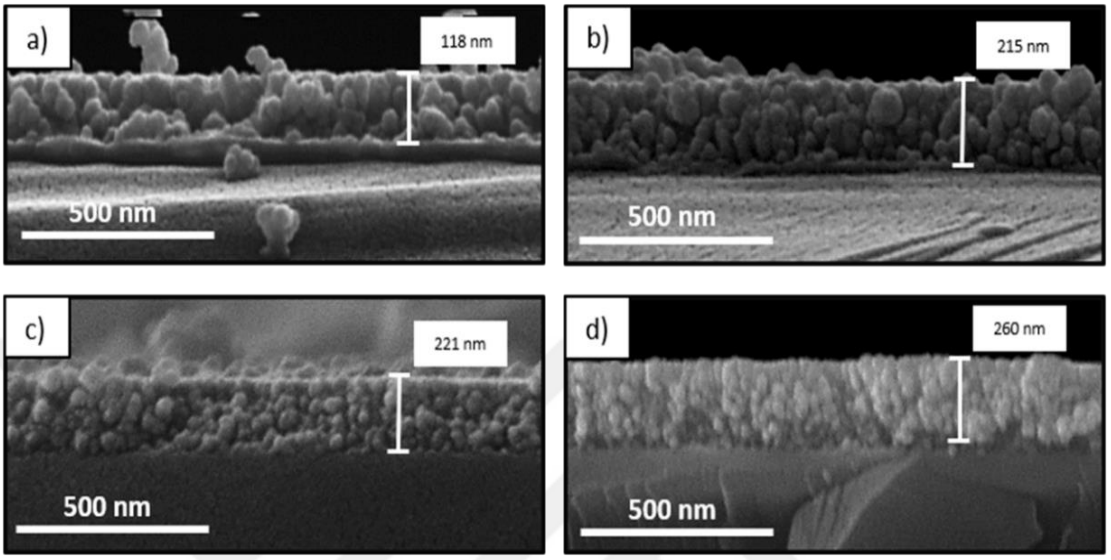

Figure 10.9: Cross-sectional SEM micrographs of undoped and 10% Ca doped ZnO thin films with spin coating method: a) undoped ZnO b) 10% Ca doped ZnO c) 3:0.5 PEG-10% Ca:ZnO d) 3:1 PEG-10% Ca:ZnO

Cross-sectional SEM micrographs of ZnO thin films (Fig. 10.9) show that the polycrystalline ZnO films have a granular structure and an average thickness of about 118, 215, 221, and 260 nm for films synthesized undoped, 10% Ca doped, 3:0.5 PEG-Ca:ZnO and 3:1 PEG -Ca:ZnO, respectively. According to the cross-sectional SEM images, the addition of Ca and PEG increased the thin film thickness.

From these figures it can be seen that the thickness of the films increases with the viscosity of the sol, which is influenced by the addition of the surfactant (PEG 400).

10.2.4. Python Analysis of Thin Films

The volume porosity values were determined using Python image processing as 29.50%, 20.66%, 9.50% and 2.20% for undoped ZnO, 10% Ca doped ZnO, 3:0.5 PEG-Ca:ZnO and 3:1 PEG-Ca:ZnO thin films, respectively. As a result, the undoped

ZnO thin films exhibit higher surface porosity than the other thin films (Fig. 10.10). Moreover, the Ca-doped ZnO films also exhibit a good porosity volume of 20.66%, with an even larger surface area compared to the undoped ZnO films.

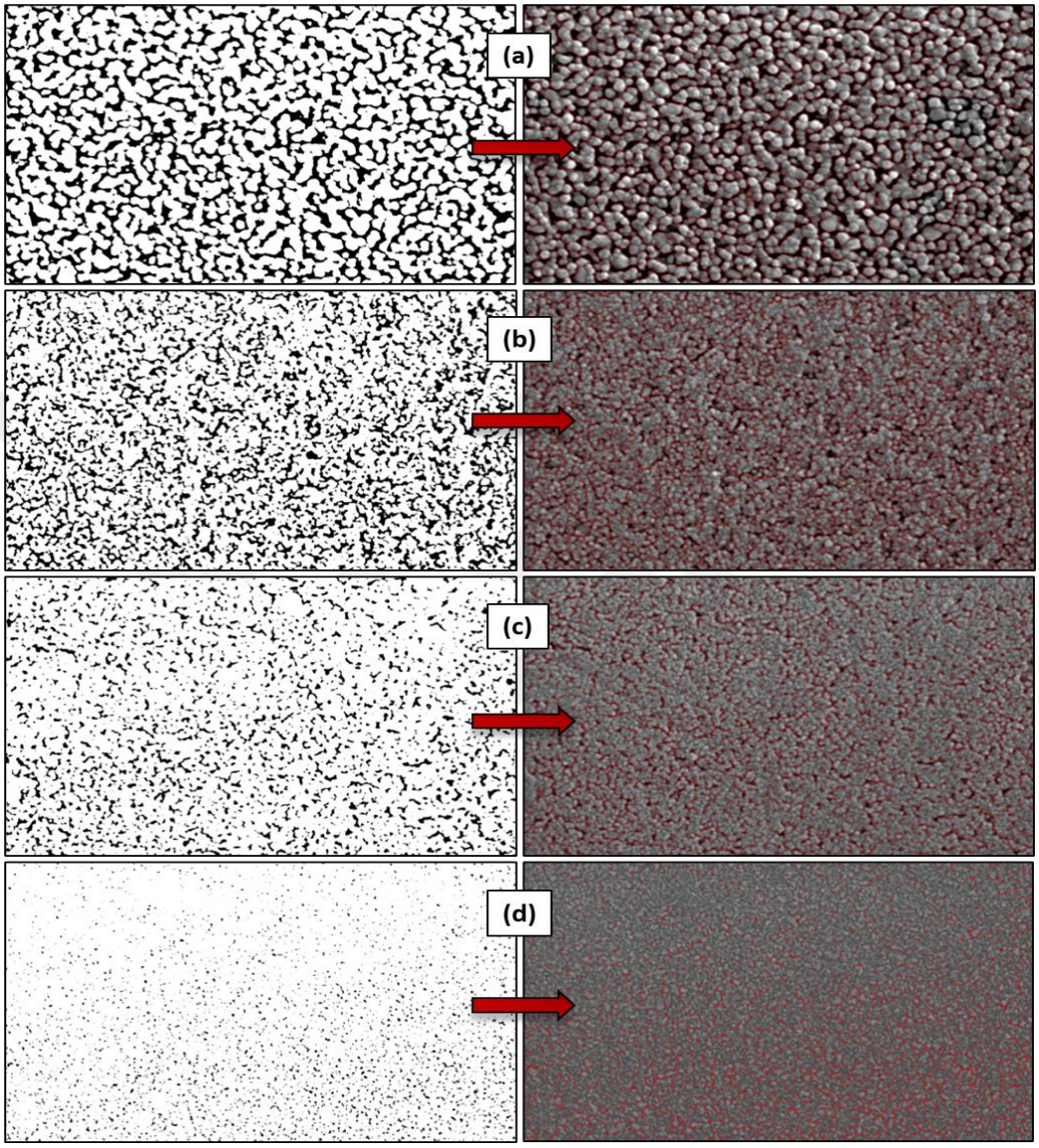

Figure 10.10: Binary images of SEM micrographs made by image processing libraries in Python as: a) undoped ZnO b) 10% Ca doped ZnO c) 3:0.5 PEG-10% Ca:ZnO d) 3:1 PEG-10% Ca:ZnO

10.2.5. UV-Vis Analysis of Thin Films

Fig. 10.11 shows the absorbance spectrum of undoped and Ca doped ZnO thin films. Strong absorption occurs as shown in Fig.10.11 in the UV wavelength at 363 nm, 350 nm, 352 nm and 354 nm for undoped, 10% Ca doped, 3:0.5 PEG-Ca:ZnO and 3:1 PEG-Ca:ZnO, respectively. The visible field between 400 and 800 nm is almost entirely covered by the weak absorption area. As can be seen from Fig. 10.11, the absorbance in the absorption spectra decreases over short wavelength ranges with 10% Ca doping (without PEG), while the Ca-doped ZnO thin film with a ZnO: PEG ratio of 3:0.5 (3:0.5 PEG -Ca:ZnO) shows higher optical absorption at all wavelengths.

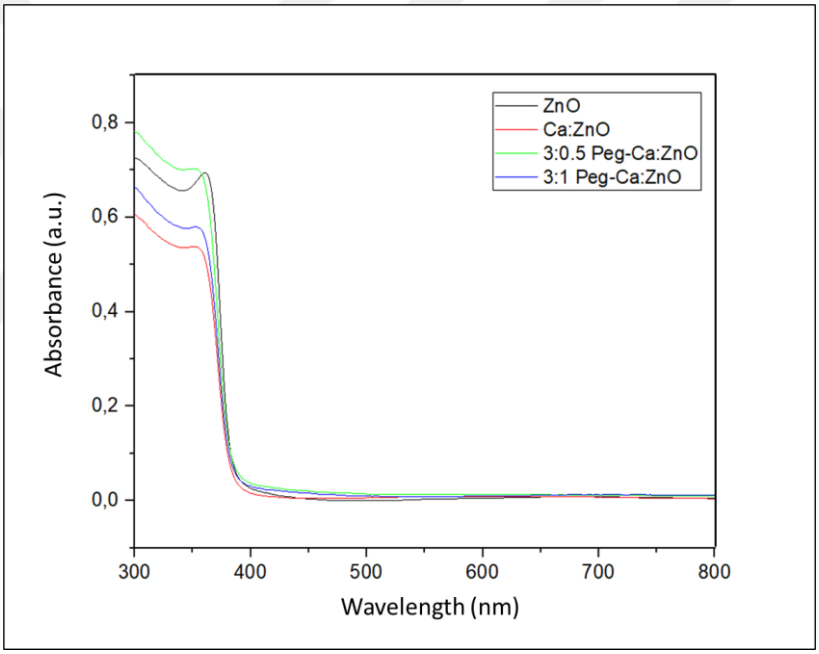

Figure 10.11: Absorption of undoped and 10% Ca doped ZnO thin films

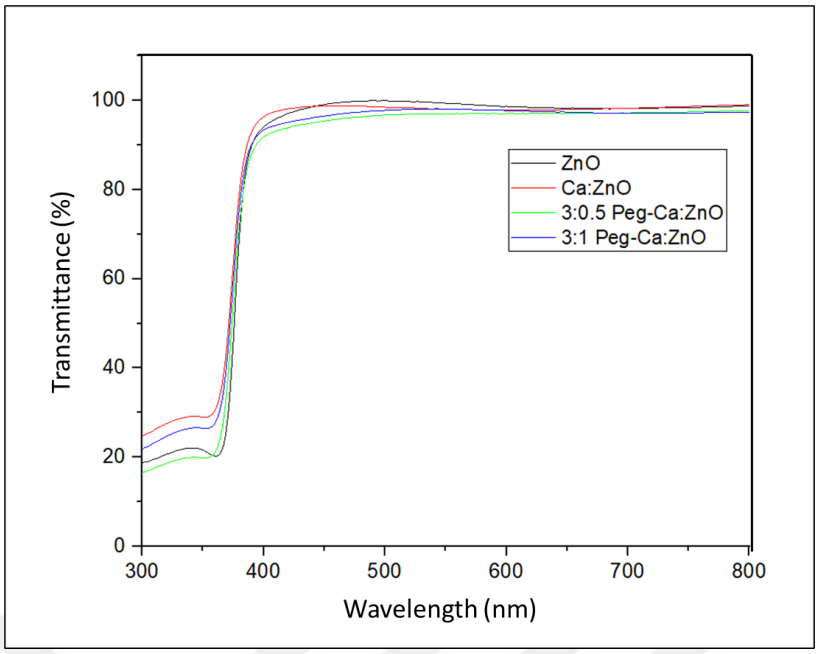

Figure 10.12: Transmittance of undoped and 10% Ca doped ZnO thin films samples

The transmittance spectrum of the undoped and 10% Ca doped ZnO thin films shown in Fig. 10.12 reveals that the transmittance of thin films in this visible region is greater than 90%.

In addition, the optical band gaps of prepared undoped and Ca doped ZnO thin films are smaller than those of bulk ZnO (3.37 eV). We have found that the optical band gap of ZnO films decreases from 3.25 eV to 3.16 eV with the doping of Ca. The optical band gap of the films was determined by their structure and atomic composition. In this study, the optical band gap of the films was strongly dependent on the Ca doping.

10.3. Microstructure and Optical Analysis of 10% Ca doped ZnO Thin Films

The 10% Ca-doped ZnO thin films were selected for use as biorecognition layers in optical biosensors due to their porous surface and optical properties. The 10% Ca-doped ZnO thin films were functionalized with APTES and GA for antibody binding. In this part of our study, we investigate unfunctionalized, APTES-GA functionalized and antibody immobilized 10% Ca-doped ZnO thin films.

10.3.1. AFM Analysis of 10% Ca doped Thin Films

The scan sizes were 5 μm x 5 μm in Fig. 10.13(a-d). The change in surface morphology after functionalization with APTES-GA of 10% Ca-doped ZnO thin films was found, and the surface roughness of APTES-GA -functionalized Ca-doped ZnO thin films was lower compared to Ca-doped ZnO thin films. For the Ca-doped ZnO sample, the average surface roughness is about 2.985 nm, while the average surface roughness of the functionalized thin films decreased to 1.164 nm. This indicates a smoothing of the surface, which can also be seen by the appearance of the surface in Fig.10.13 (c). In this study, we functionalized our thin films with 2% concentration of APTES. Kim et al. developed indium gallium zinc oxide (IGZO) thin films functionalized with 1%, 5% and 17% APTES concentration. At 5% APTES concentration, the peaks decreased rapidly and the morphology was smoother than at 1% [119].

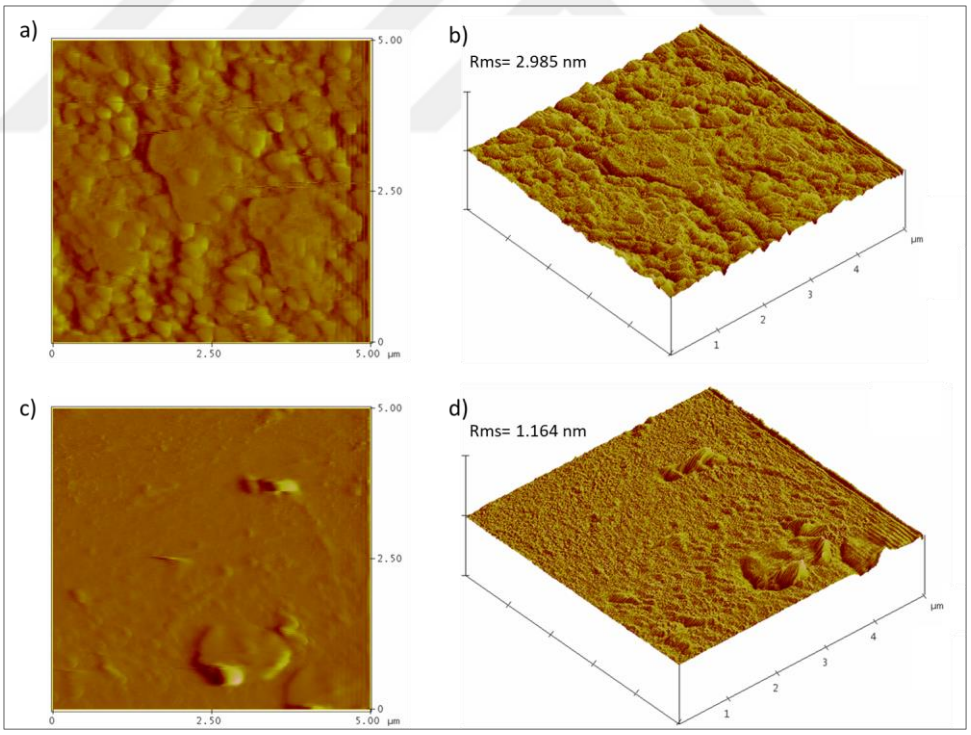

Figure 10.13: a-b) Unfunctionalized and c-d) Functionalized AFM topography images of 10% Ca doped ZnO thin film

10.3.2. UV-Vis Analysis of 10% Ca doped Thin Films

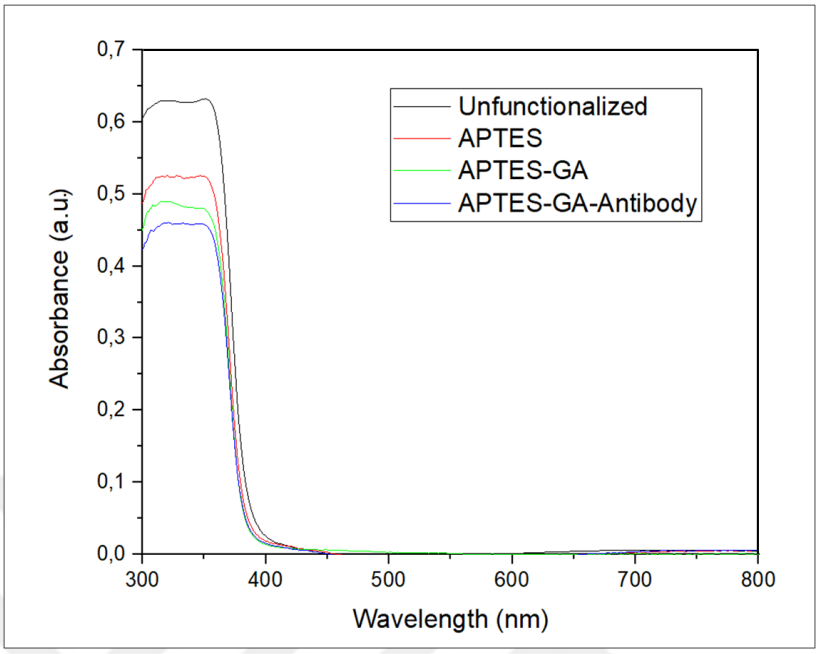

Figure 10.14: Absorbance of unfunctionalized, functionalized with APTES-GA and antibody immobilized thin films

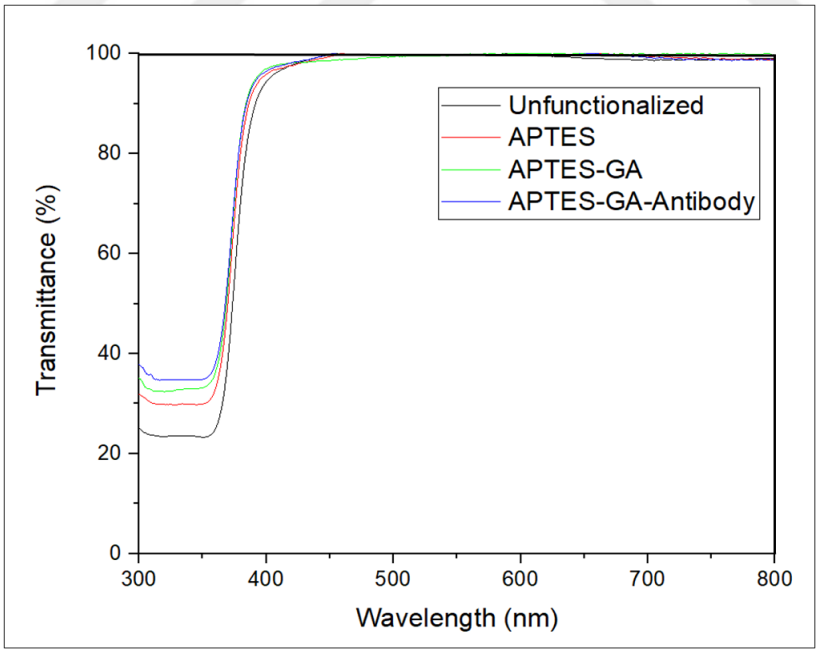

Figure 10.15: Transmittance of unfunctionalized, functionalized with APTES-GA and antibody immobilized thin films

Functionalized 10% Ca doped ZnO thin films absorb in the same wavelength range as unfunctionalized thin films, but the corresponding absorption is lower. That

is, after the surface is modified with APTES-GA, the UV absorption of the functionalized Ca:ZnO films decreases, as shown in Fig. 10.14. This result is in agreement with the results of Jaramillo et al. [120]. Absorption value of antibody immobilized thin film is approximately 27.5% lower than the unfunctionalized thin film between the 300-360 nm. The antibody-bound surface has the lowest absorbance value in the same wavelength range. The transmittance spectrum of non-functionalized and functionalized Ca:ZnO thin films shown in Fig. 10.15 indicates that the thin films have a transmittance of more than 90% in this visible region.

10.4. Ca Doped ZnO Thin Films Integrated with UV-Vis Instrument as an Optical Biosensors for Bisphenol A (BPA) Detection

UV-VIS spectroscopy as an optical transducer was used to detect four different concentrations of BPA based on changes in absorbance values. As shown in Fig. 10.16, the optical absorption of the Ca:ZnO thin films decreases with increasing BPA concentration. The differences in the logarithmic absorbance values obtained for the sensor after interaction with different BPA concentrations are shown in Fig. 10.16. UV-Vis measurements were performed in a concentration range of 50-300 ng/ml BPA. The limit of detection (LOD) value was calculated according to equation (10.1):

$$LOD = C_0 + k \times S_0 \tag{10.1}$$

where C_0 is the mean concentration of the blank solution measurements, S_0 is the standard deviation of the blank solution measurements, and k is a specific numerical factor based on the desired confidence level (95% confidence level, k=3) [121]. The detection limit of BPA was found to be 0.49 μg/ml. In the literature, there are studies on optical biosensors using antibodies as a receptor for the detection of BPA. For example, Hegnerová et. al. reported the SPR biosensor probe with a detection limit of 0.08 ng/ml for the detection of BPA in PBS [122]. In another study using the antibody as a receptor, LOD was determined to be 40 pg/ml for BPA [123]. Rodriguez-Mozaz et al. developed an optical biosensor based on total internal reflection fluorescence, which was LOD of 14 ng/L [124].

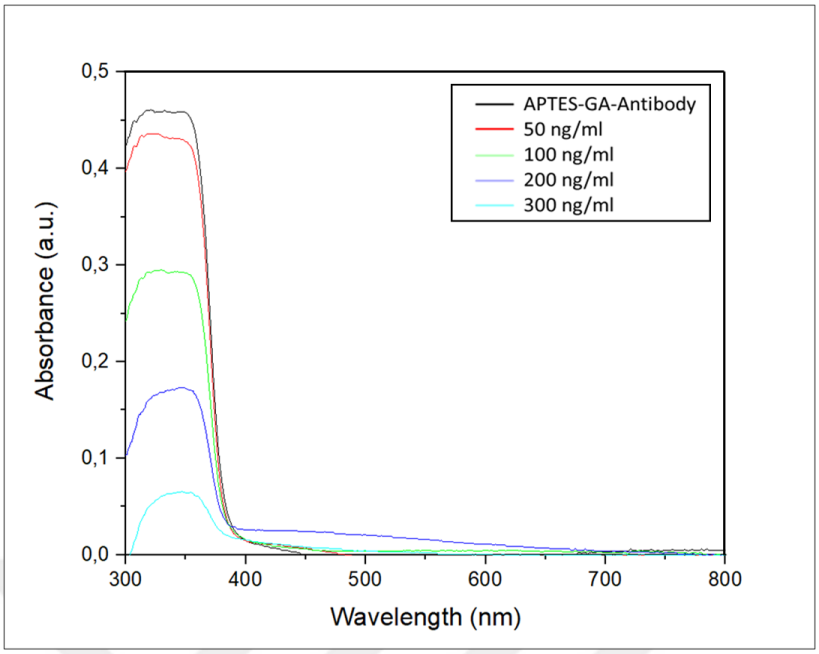

Figure 10.16: Absorbance measurements in different BPA concentrations

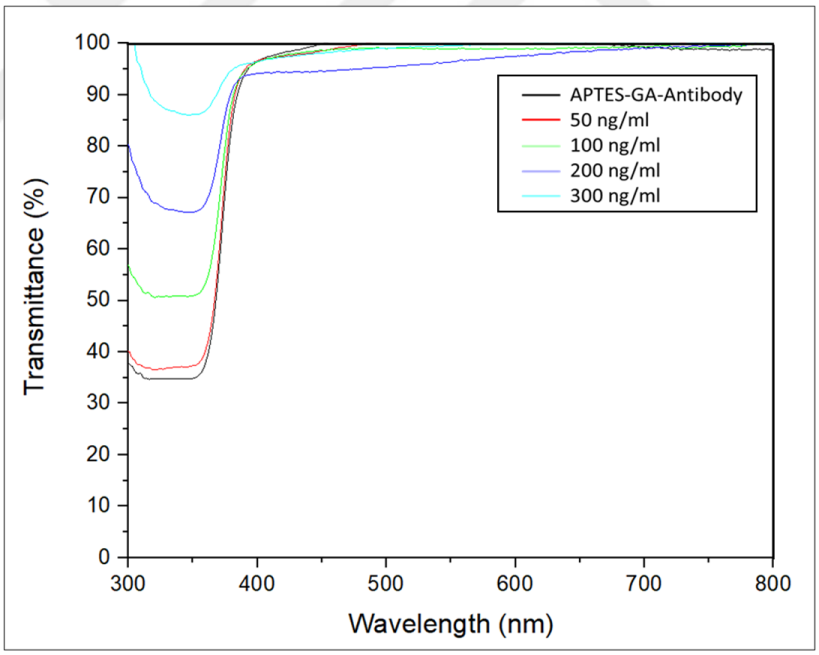

Figure 10.17: Transmittance measurements in different BPA concentrations

Fig. 10.17 shows the transmission measurements for different BPA concentrations in the linear dynamic range. After functionalization and immobilization, the transmittance values of the Ca:ZnO thin films did not change significantly in this visible range.

11. CONCLUSION

ZnO and Ca-doped ZnO thin films with a concentration of 0.5 molarities were deposited on glass substrates by sol-gel method using two different techniques: dip coating and spin coating technique. We successfully incorporated Ca into the ZnO lattice and examined changes in the surface morphology (e.g., the ratio of surface porosity and particle size), structural parameters (e.g., average crystal size), and optical properties (e.g., volume porosity, refractive index, band gap, and transmittance). The surface of the Ca-doped ZnO thin films was functionalized with APTES to be used for optical biosensor applications. After the functionalization process, a polyclonal BPA antibody was immobilized on the functionalized surfaces to detect the chemical BPA. The detection of BPA was successfully performed using a UV-Vis-NIR spectroscopy instrument.

According to the XRD results, the studied thin films and powder samples were polycrystalline and consisted of ZnO nanocrystals with hexagonal zincite phase. The calcite phase was also found in the powder sample spiked with Ca, unlike in the thin films. It was concluded that the crystal size decreased with the addition of Ca and PEG in the films obtained according to Scherrer equation.

In the SEM results, it was found that the deposited films were uniformly doped with Ca, which led to a decrease on the crystal size. The highest pore ratio was found in both the undoped and 10% Ca-doped ZnO films, as shown by the python image processing results of the SEM images. It was also observed that the pore size decreased in the Ca-doped ZnO thin films in SEM images, implying that the surface area to volume ratio of the thin films was increased for immobilization of more biomolecules.

The refractive indices of the thin films produced by the dip coating method were measured with a prism coupler with high precision and low standard deviation. The theoretical refractive indices of the thin films were calculated using the formula, and an average porosity calculation for the thin films was performed by comparing the theoretical refractive indices with the refractive indices obtained by the prism coupler results.

UV-Vis-NIR spectroscopy has been used both to measure the optical properties of thin films by spin coating and to detect the chemical BPA as a transducer in optical biosensors. In the visible region of the optical spectrum, all ZnO films have a high

average transmittance of more than 90%. All films exhibited strong absorption below 400 nm. UV-Vis results showed that incorporation of Ca decreases the optical absorption of ZnO thin films. 10% Ca-doped ZnO thin films were selected as a suitable surface for antibody binding because the nanoporous structure of the 10% Ca-doped ZnO thin films is particularly good compared to other thin films. Therefore, the functionalization and immobilization processes were carried out on this film surface. After APTES-GA functionalization and immobilization of anti-BPA antibodies, the following decrease in optical absorbance of each process was detected by UV-Vis-NIR spectrophotometer. Finally, the UV-Vis spectrophotometer was used to detect different BPA concentrations between 50 ng/ml and 300 ng/ml. The detection limit of this probe was set at 0.49 μg/ml. In the literature, there are more sensitive optical sensors for the detection of BPA in nanogram and picogram concentrations. This study can be considered as a preliminary study since a novel biorecognition layer and UV-vis spectrophotometer were used as a new optical detection method for BPA. Therefore, our LOD results were quite reasonable compared to the other studies.

Biosensors and their biomedical applications are gaining increasing attention for early detection of diseases and tracking the body's response to treatment. The improvement of biosensors as an analytical device has prompted researchers to investigate various materials with unique optical and electrical properties, biocompatibility, cost-effectiveness, and ease of fabrication. These results show that porous 10% Ca-doped ZnO thin films can be a good candidate for optical biosensors. In this regard, these simple, inexpensive, and biocompatible films can be easily integrated into optical devices and can be preferred as a biorecognition layer in optical biosensors to detect various types of diseases caused by viruses, bacteria, or cancer cells in health care.

REFERENCES

[1] Mehrotra P., 2016, "Biosensors and their applications – A review", Journal of Oral Biology and Craniofacial Research, 6 (2),153-159.

[2] Bhalla N., Jolly P., Formisano N., Estrela P., (2016), "Introduction to biosensors", Essays Biochem., 60 (1),1–8.

[3] Patel S., Nanda R., Sahoo S., Mohapatra E., (2016), "Biosensors in health care: The milestones achieved in their development towards lab-on-chip-analysis", Biochem. Res. Int.

[4] Mir T. A., Faisal K., Hospital S., Abrahim S., Nawaz, A., (2015), "Biosensors and their biomedical applications : Invited Review Biosensors and their biomedical applications", Journal of Pharmacy and Pharmaceutical Sciences, 3 (2).

[5] Manikandan R., Charumathe N. Begum A. F., (1992), "Application of Biosensors", Tech. Instrum. Anal. Chem.,11 (100), 291–322.

[6] Metkar S. K., Girigoswami K., (2019), "Diagnostic biosensors in medicine – A review", Biocatal. Agric. Biotechnol., 17, 271–283.

[7] Vigneshvar S., Sudhakumari C. C., Senthilkumaran B., Prakash H., (2016), "Recent advances in biosensor technology for potential applications - an overview", Front. Bioeng. Biotechnol., 4,1–9.

[8] Damborský P., Švitel J., Katrlík J., (2016), "Optical biosensors", Essays Biochem., 60 (1), 91–100.

[9] Garzón V., Pinacho D. G., Bustos R. H., Garzón G., Bustamante S., (2019), "Optical biosensors for therapeutic drug monitoring", Biosensors, 9 (4), 1–26.

[10] Arya S. K., Saha S., Ramirez-Vick J. E., Gupta V., Bhansali S., Singh S. P., (2012), "Recent advances in ZnO nanostructures and thin films for biosensor applications: Review", Anal. Chim. Acta, 737,1–21.

[11] Law W. C., Yong K. T., Baev A., Prasad P. N., (2011), "Sensitivity improved surface plasmon resonance biosensor for cancer biomarker detection based on plasmonic enhancement", ACS Nano, 5 (6), 4858–4864.

[12] Choi B. G., Park H., Park T. J., Yang M. H., Kim J. S., Jang S-Y., Heo N. S., Lee S. Y., Kong J., Hong W. H., (2010), "Solution Chemistry of Self-Assembled Graphene Nanohybrids for High-Performance Flexible Biosensors", 4 (5), 2910–2918.

[13] Choi J. W., Oh B. K., Kim Y. K., Min J., (2007), "Nanotechnology in biodevices", J. Microbiol. Biotechnol., 17 (1), 5–14.

[14] Karim S. S. A., Dee C. F., Majlis B. Y., Mohamed M. A., (2019), "Recent progress on fabrication of zinc oxide nanorod-based field effect transistor biosensors", Sains Malaysiana, 48 (6), 1301–1310.

[15] Istrate A-I., Nastase F., Mihalache I., Comanescu F., Gavrila R., Tutunaru O., Romanitan C., Tucureanu V., Nedelcu V., Müller R., (2019), "Synthesis and characterization of Ca doped ZnO thin films by sol–gel method", J. Sol-Gel Sci. Technol., 92 (3), 585–597.

[16] Huang L., Guo Y., Peng Z., Porter A. L., (2011), “Characterising a technology development at the stage of early emerging applications: Nanomaterial-enhanced biosensors”, Technol. Anal. Strateg. Manag., 23 (5), 527–544.

[17] Singh S.,Kumar V., Dhanjal D. S., Datta S., Prasad R., Singh J., (2020), “Biological Biosensors for Monitoring and Diagnosis”, 317–335.

[18] Shaheen A., Arshad R., Taj A., Latif U., Bajwa S. Z., (2020), “Biosensor Applications for Viral and Bacterial Disease Diagnosis”, Nanobiosensors, 117–148.

[19] Huang Y., Xu, J., Liu, J., Wang X., Chen B., (2017), “Disease-related detection with electrochemical biosensors: A review”, Sensors, 17 (10), 1–30.

[20] Haleem A., Javaid M., Singh R. P., Suman R., Rab S., (2021), “Biosensors applications in medical field: A brief review”, Sensors Int., 2, 100100.

[21] Rodovalho V. R., Alves L. M, Castro A.C.H., Madurro J.M., Brito-Madurro A.G., and Santos A.R., (2015), “Biosensors Applied to Diagnosis of Infectious Diseases – An Update”, Austin J. Biosens. Bioelectron., 1 (3), 1–12.

[22] Thévenot D. R., Toth K., Durst R. A., Wilson G. S., (2001), “Electrochemical biosensors: Recommended definitions and classification”, Biosens. Bioelectron., 16 (1-2), 121–131.

[23] Lynn N. S., Šípová H., Adam P., Homola J., (2013), “Enhancement of affinity-based biosensors: Effect of sensing chamber geometry on sensitivity”, Lab Chip, 13 (7), 1413–1421.

[24] Njagi J. I., Kagwanja S. M., (2011), “The interface in biosensing: Improving selectivity and sensitivity”, ACS Symp. Ser., 1062, 225–247.

[25] Dak P., Ebrahimi A., Swaminathan V., Duarte-Guevara C., Bashir R., Alam M., (2016), “Droplet-based biosensing for lab-on-a-chip, open microfluidics platforms”, Biosensors, 6 (2), 16–21.

[26] Karunakaran C., Rajkumar R., Bhargava K., (2015), "Introduction to Biosensors". In: C. Karunakaran, K. Bhargava, R. Banjamin, Editors, "Biosensors and Bioelectronics", Elsevier Inc., 2015

[27] Naresh V., Lee N., (2021), “A review on biosensors and recent development of nanostructured materials-enabled biosensors”, Sensors (Switzerland), 21 (4), 1–35.

[28] Alhadrami H. A., (2018), “Biosensors: Classifications, medical applications, and future prospective”, Biotechnol. Appl. Biochem., 65 (3), 497–508.

[29] Velusamy V., Arshak K., Korostynska O., Oliwa K., Adley C., (2010), “An overview of foodborne pathogen detection: In the perspective of biosensors”, Biotechnol. Adv., 28 (2), 232–254.

[30] Pearson J. E., Gill A., Vadgama P., (2000), “Analytical aspects of biosensors”, Ann. Clin. Biochem., 37 (2), 119–145.

[31] Khansil N., Rattu G., Krishna P. M., (2018), “Label-free optical biosensors for food and biological sensor applications”, Sensors Actuators, B Chem., 265, 35–49.

[32] Chen C., Wang J., (2020), “Optical biosensors: An exhaustive and comprehensive review”, Analyst, 145 (5), 1605–1628.

[33] Masson J. F., (2017), “Surface Plasmon Resonance Clinical Biosensors for Medical Diagnostics”, ACS Sensors, 2 (1), 16–30.

[34] Liu J., Jalali M., Mahshid S., Wachsmann-Hogiu S., (2020), “Are plasmonic optical biosensors ready for use in point-of-need applications?”, Analyst, 145 (2), 364–384.

[35] Hammond J. L., Bhalla N., Rafiee S. D., Estrela P., (2014), “Localized surface plasmon resonance as a biosensing platform for developing countries”, Biosensors, 4 (2), 172–188.

[36] Wang J., Dong J., (2020), “Optical Waveguides and Integrated Optical Devices for Medical Diagnosis, Health Monitoring and Light Therapies”, 20 (14), 3981.

[37] Purohit B., Vernekar P. R., Shetti N. P., Chandra P., (2020), “Biosensor nanoengineering: Design, operation, and implementation for biomolecular analysis”, Sensors Int., 1,100040.

[38] Zhu Y., Qu C., Kuang H., Xu L., Liu L., Hua Y., Wang L., Xu C., (2011), “Simple, rapid and sensitive detection of antibiotics based on the side-by-side assembly of gold nanorod probes”, Biosens. Bioelectron., 26 (11), 4387–4392.

[39] Que X., Tang D., Xia B., Lu M., Tang D., (2014), “Gold nanocatalyst-based immunosensing strategy accompanying catalytic reduction of 4-nitrophenol for sensitive monitoring of chloramphenicol residue”, Anal. Chim. Acta, 830, 42–48.

[40] Balakrishnan G., Sinha V., Peethala P. Y., Kumar M., Golden Renjit Nimal, N.J., Hameed Husseyin J., Batoo, K. M., Raslan, E. H., (2014), “Structural and optical properties of ZnO thin film prepared by sol-gel spin coating”, Mater. Sci. Pol., 38 (1), 17–22.

[41] Cho I. H., Kim D. H., Park S., (2020), “Electrochemical biosensors: Perspective on functional nanomaterials for on-site analysis”, Biomater. Res., 24 (1), 1–12.

[42] Pandey C. M., Malhotra B. D., (2019), "Biosensors: Fundamentals and applications", 2nd Edition, De Gruyter.

[43] Chaubey A., Malhotra B. D., (2002), “Review Mediated biosensors”, Biosens. Bioelectron.,7, 441–456.

[44] Walker N. L., Roshkolaeva A. B., Chapoval A. I., Dick J. E., (2021), “Recent advances in potentiometric biosensing”, Curr. Opin. Electrochem., 28, 100735.

[45] Mousavi M. P. S., Abd El-Rahman M. K., Mahmoud A. M., Abdelsalam R. M., Bühlmann P., (2018), “In Situ Sensing of the Neurotransmitter Acetylcholine in a Dynamic Range of 1 nM to 1 mM”, 3 (12), 2581–2589.

[46] Ibupoto Z. H., Jamal N., Khun K., Willander M., (2012), “Development of a disposable potentiometric antibody immobilized ZnO nanotubes based sensor for the detection of C-reactive protein”, Sensors Actuators, B Chem., 166–167, 809–814.

[47] Hernández R., Vallés C., Benito A. M., Maser W. K., Xavier Rius F., Riu J., (2014), “Graphene-based potentiometric biosensor for the immediate detection

of living bacteria", Biosens. Bioelectron., 54, 553–557.

[48] Soldatkina O. V., Kucherenko I. S., Soldatkin O. O., Pyeshkova V. M., Dudchenko O. Y., Akata Kurç B., Dzyadevych S. V. (2019), "Development of electrochemical biosensors with various types of zeolites", Appl. Nanosci., 9 (5), 737–747.

[49] Odobašić A., Šestan I., Begić S., (2019), "Biosensors for Determination of Heavy Metals in Waters", Biosens. Environ. Monit.

[50] Belluzo M. S., Ribone M. É., Lagier C. M., (2008), "Assembling amperometric biosensors for clinical diagnostics", Sensors, 8 (3), 1366–1399.

[51] Grieshaber D., MacKenzie R., Vörös J., Reimhult E., (2008), "Electrochemical biosensors - Sensor principles and architectures", Sensors, 8 (3), 1400–1458.

[52] Okafor C., Grooms D., Alocilja E., Bolin S., (2008), "Fabrication of a novel conductometric biosensor for detecting Mycobacterium avium subsp. paratuberculosis antibodies", Sensors, 8 (9), 6015–6025.

[53] Malhotra B. D., Ali M. A., (2018), "Nanomaterials in Biosensors", Nanomaterials for Biosensors, 1–74.

[54] Zhang S., Wright G., Yang Y., (2000), "Materials and techniques for electrochemical biosensor design and construction", Biosens. Bioelectron., 15 (5-6), 273–282.

[55] Sandulescu R., Tertis M., Cristea C., Bodoki E., (2015), "New Materials for the Construction of Electrochemical Biosensors", Biosens. - Micro Nanoscale Appl., 1–36.

[56] Xie B., Danielsson B., (2008), "Thermal Biosensor and Microbiosensor Techniques", Handb. Biosens. Biochips.

[57] Wang L., Sipe D. M., Xu Y., Lin Q., (2008), "A MEMS thermal biosensor for metabolic monitoring applications", J. Microelectromechanical Syst., 17 (2), 318–327.

[58] Lu P., Zhang D., Chai Y., Yu C., Wang X., Tang Y., Ge M., Yao L., (2019), "Regulatory-sequence mechanical biosensor: A versatile platform for investigation of G-quadruplex/label-free protein interactions and tunable protein detection", Anal. Chim. Acta, 1045, 1–9.

[59] Fritz J., (2008), "Cantilever biosensors", Analyst, 133 (7), 855–863.

[60] Tamayo J., Kosaka P. M., Ruz J. J., Paulo Á. S., Calleja M., (2013), "Biosensors based on nanomechanical systems", Chem. Soc. Rev., 42 (3), 1287–1311.

[61] Scheller F. W., Wollenberger U., Warsinke A., Lisdat F., (2001), "Research and development in biosensors", Curr. Opin. Biotechnol., 12 (1), 35–40.

[62] Nguyen H. H., Lee S. H., Lee U. J., Fermin C. D., Kim M., (2019), "Immobilized enzymes in biosensor applications", Materials (Basel)., 12 (1), 1–34.

[63] Liu A., Wang K., Weng S., Lei Y., Lin L., Chen W., Lin X., Chen Y., (2012), "Development of electrochemical DNA biosensors", TrAC - Trends Anal. Chem., 37, 101–111.

[64] Zhu Q., Liu G., Kai M., Miller A. O. A., (2015), “DNA aptamers in the diagnosis and treatment of human diseases”, Molecules, 20 (12), 20979–90997.

[65] Kaur H., Bhosale A., Shrivastav S., (2018), “Biosensors: Classification, Fundamental Characterization and New Trends: A Review”, Int. J. Heal. Sci. Res., 8 (6), 315–333.

[66] Endo S. B. I., Hu S. E. W., Nielsen B. M. J., Tsao G. S. G., Zeng T. R. U. A., Zhou J. Z. W., (2010), "Advances in Biochemical Engineering/Biotechnology".

[67] Schmidt J. J., Montemagno C. D., (2004), “Bionanomechanical systems”, Annu. Rev. Mater. Res., 34, 315–337.

[68] Song M., Lin X., Peng Z., Xu S., Jin L., Zheng X., Luo H., (2021), “Materials and Methods of Biosensor Interfaces With Stability”, Front. Mater., 7, 1–11.

[69] Prieto-Simon B., Campas M., Marty J.-L., (2008), “Biomolecule Immobilization in Biosensor Development: Tailored Strategies Based on Affinity Interactions”, Protein Pept. Lett., 15 (8), 757–763.

[70] Asal M., Özen Ö., Şahinler M., Baysal H. T., Polatoğlu İ., (2019), “An overview of biomolecules, immobilization methods and support materials of biosensors”, Sens. Rev., 39 (3), 377–386.

[71] Nimse S. B., Song K., Sonawane M. D., Sayyed D. R., Kim T., (2014), “Immobilization techniques for microarray: Challenges and applications”, Sensors (Switzerland), 14 (12), 22208–22229.

[72] Liébana S., Drago G. A., (2016), “Bioconjugation and stabilisation of biomolecules in biosensors”, Essays Biochem., 60 (1), 59–68.

[73] Nguyen H. H., Kim M., (2017), “An Overview of Techniques in Enzyme Immobilization”, Appl. Sci. Converg. Technol., 26 (6), 157–163.

[74] Javed M. R., Ibrahim M., Hussain K., Nadeem H., (2019), “Methods of Enzyme Immobilization on Various Supports”, Enzymatic Fuel Cells – Materials and Applications, 1–28.

[75] Sassolas A., Blum L. J., Leca-Bouvier B. D., (2012), “Immobilization strategies to develop enzymatic biosensors”, Biotechnol. Adv., 30 (3), 489–511.

[76] Roy I., Gupta M. N., (2006), “Bioaffinity Immobilization”, 1, 107–116.

[77] Makaraviciute A., Ramanaviciene A., (2013), “Site-directed antibody immobilization techniques for immunosensors”, Biosens. Bioelectron., 50, 460–471.

[78] Bezbaruah A. N., Kalita H., (2010), "Sensors and biosensors for endocrine disrupting chemicals : State-of-the-art and future trends", 93-127.

[79] Eltzov E., Kushmaro A., Marks R. S., (2009), "Biosensors for endocrine disruptors", Endocrine-Disrupting Chemicals in Food, Woodhead Publishing Series in Food Science, Technology and Nutrition, 183-208.

[80] Varmira K., Saed-Mocheshi M., Jalalvand A. R., (2017), “Electrochemical sensing and bio-sensing of bisphenol A and detection of its damage to DNA”, Sens. Bio-Sensing Res., 5, 7–33.

[81] Yilmaz B., Terekeci H., Sandal S., Kelestimur F., (2020), "Endocrine disrupting chemicals: exposure, effects on human health, mechanism of action, models for testing and strategies for prevention", Rev. Endocr. Metab. Disord., 21 (1), 127–147.

[82] Ragavan K. V., Rastogi N. K., Thakur M. S., (2013), "Sensors and biosensors for analysis of bisphenol-A", TrAC - Trends Anal. Chem., 52, 248–260.

[83] Rubin B. S., (2011), "Bisphenol A: An endocrine disruptor with widespread exposure and multiple effects", J. Steroid Biochem. Mol. Biol., 127 (1-2), 27–34.

[84] Yildirim-Tirgil N., Long F., He M., Shi H., Gu A. Z., (2014), "A portable optic fiber aptasensor for sensitive, specific and rapid detection of bisphenol-A in water samples", Environmental Science: Processes and Impacts, 16 (6).

[85] Xiong Y., Ye Z., Xu J., Liu Y., Zhang H., (2014), "A microvolume molecularly imprinted polymer modified fiber-optic evanescent wave sensor for bisphenol A determination", Anal. Bioanal. Chem., 406 (9-10), 2411–2420.

[86] Luo H., Lin X., Peng Z., Song M., Jin, L., (2020), "Rapid and sensitive detection of bisphenol a based on self-assembly", Micromachines, 11 (1), 41.

[87] Nazari M., Kashanian S., Rafipour R., Omidfar K., (2019), "Biosensor design using an electroactive label-based aptamer to detect bisphenol A in serum samples", J. Biosci., 44 (4),1–10.

[88] Liu Y., Yao L., He L., Liu N., Piao, Y., (2019), "Electrochemical enzyme biosensor bearing biochar nanoparticle as signal enhancer for bisphenol a detection in water", Sensors (Switzerland), 19 (7),1619.

[89] Sheng W., Duan W., Shi Y., Chang Q., Zhang Y., Lu Y., Wang S., (2018), "Sensitive detection of bisphenol A in drinking water and river water using an upconversion nanoparticles-based fluorescence immunoassay in combination with magnetic separation", Anal. Methods,10 (44),5313–5320.

[90] Xue C. S., Erika G., Jiří H., (2019), "Surface plasmon resonance biosensor for the ultrasensitive detection of bisphenol A", Anal. Bioanal. Chem., 411 (22), 5655–5658.

[91] Tereshchenko A., Bechelany M., Viter R., Khranovskyy V., Smyntyna V., Starodub N., Yakimova R., (2016), "Optical biosensors based on ZnO nanostructures: Advantages and perspectives. A review", Sensors Actuators, B Chem., 229, 664–677.

[92] Malek M. F., Mamat M. H., Zahidi M. M., Sahdan M. Z., Mahmood, M. R., (2016), "Factors affecting the properties of zinc oxide thin films prepared by dip-coating method", Adv. Mater. Res., 667, 193–199.

[93] Durán Retamal J. R., Lien W. C., He H., (2012), "Biosensing applications of ZnO nanostructures", Handb. Innov. Nanomater. From Synth. to Appl., 665–692.

[94] Wei A., Pan L., Huang W., (2011), "Recent progress in the ZnO nanostructure-based sensors", Mater. Sci. Eng. B Solid-State Mater. Adv. Technol., 176 (18), 1409–1421.

[95] Mahmood A., Naeem A., (2017), "Sol-Gel-Derived Doped ZnO Thin Films:

Processing, Properties, and Applications", Recent Appl. Sol-Gel Synth.

[96] Norton D. P., Heo Y. W., Ivill M. P., Pearton S. J., Chisholm M, F., Steiner T. D., (2004), "ZnO: growth, doping and processing", Mater. today, 7 (6), 34–40.

[97] Kahraman S., Çakmak H. M., Çetinkaya S., Bayansal F., Çetinkara H. A., Güder H. S., (2013), "Characteristics of ZnO thin films doped by various elements", J. Cryst. Growth, 363, 86–92.

[98] Kunene K., Sabela M., Kanchi S., Bisetty K., (2020), "High Performance Electrochemical Biosensor for Bisphenol A Using Screen Printed Electrodes Modified with Multiwalled Carbon Nanotubes Functionalized with Silver-Doped Zinc Oxide", Waste and Biomass Valorization, 11 (3),1085–1096.

[99] Qiao Y., Li J., Li H., Fang H., Fan D., Wang W., (2016), "A label-free photoelectrochemical aptasensor for bisphenol A based on surface plasmon resonance of gold nanoparticle-sensitized ZnO nanopencils", Biosens. Bioelectron., 86, 315–320.

[100] Zhang J., Zhao S. Q., Zhang K., Zhou J. Q., (2014), "Cd-doped ZnO quantum dots-based immunoassay for the quantitative determination of bisphenol A", Chemosphere, 95, 105–110.

[101] Hench L. L., West J. O. N. K., (1990), "The Sol-Gel Process", 33–72.

[102] Wang X., (2020), "Preparation , synthesis and application of Sol-gel method".

[103] Znaidi L., (2010), "Sol-gel-deposited ZnO thin films: A review", Mater. Sci. Eng. B Solid-State Mater. Adv. Technol., 174 (1–3), 18–30.

[104] Khan N., (2001), "History of science and technology", Bull. Sci. Technol. Soc., 21 (6), 510.

[105] Nisticò R., Scalarone D., Magnacca G., (2017), "Sol-gel chemistry, templating and spin-coating deposition: A combined approach to control in a simple way the porosity of inorganic thin films/coatings", Microporous Mesoporous Mater., 248, 18–29.

[106] John D., Wright N. A. J. M. S., (2000), "Sol-Gel Materials Chemistry and Applications", 148.

[107] Esposito S., (2019), "'Traditional' sol-gel chemistry as a powerful tool for the preparation of supported metal and metal oxide catalysts", Materials (Basel)., 12 (4), 1–25.

[108] Ye Q., (2013), "Sol-Gel Processes of Functional Powders and Films", Web Sci., 31-50.

[109] Guglielmi M., (1990), "Sol-gel science", Materials Chemistry and Physics, 26 (2), 211–212.

[110] Landau M. V., (2008), "Sol–Gel Process", Handbook of Heterogeneous Catalysis, 119-159.

[111] Aguilar G. V., (2019), "A Brief Semblance of the Sol-Gel Method in Research", Sol-Gel Method - Design and Synthesis of New Materials with Interesting Physical, Chemical and Biological Properties, 3–8.

[112] Brinker C. J., Hurd A. J., Schunk P. R., Frye G. C., Ashley C. S., (1992), "Review of sol-gel thin film formation", J. Non. Cryst. Solids, 147–148, 424–436.

[113] Nagyal L., Gupta S. S., Singh R., Kumar A., Chaudhary P., (2019), "Sol – Gel Deposition of Thin Films", 1–18.

[114] Scriven L. E., (1988), "Physics and Applications of DIP Coating and Spin Coating", MRS Proc., 121, 717–729.

[115] Wang C. T., Yen S. C., (1995), "Theoretical analysis of film uniformity in spinning processes", Chem. Eng. Sci., 50 (6), 989–999.

[116] Munje R. D., Jacobs M., Muthukumar S., Quadri B., Shanmugam N. R., Prasad S., (2015), "A novel approach for electrical tuning of nano-textured zinc oxide surfaces for ultra-sensitive troponin-T detection", Anal. Methods, 7 (24), 10136–10144.

[117] Hazzazi F., Young A., O'loughlin C., Daniels-Race T., (2021), "Fabrication of zinc oxide nanoparticles deposited on (3-aminopropyl) triethoxysilane-treated silicon substrates by an optimized voltage-controlled electrophoretic deposition and their application as fluorescence-based sensors", Chemosensors, 9 (1), 1–13.

[118] Santangelo S., Patanè S., Frontera P., Pantò F., Triolo C., Stelitano S., Antonucci P., (2017), "Effect of calcium- and/or aluminum-incorporation on morphological, structural and photoluminescence properties of electro-spun zinc oxide fibers", Mater. Res. Bull., 92, 9–18.

[119] Kim H., Kwon J. Y., (2017), "Enzyme immobilization on metal oxide semiconductors exploiting amine functionalized layer", RSC Adv., 7 (32), 19656–19661.

[120] Jaramillo A. F., Baez-Cruza R., Montoya L. F., Medinam C., Pérez-Tijerina E., Salazar F., Rojas D., Melendrez M. F., (2017), "Estimation of the surface interaction mechanism of ZnO nanoparticles modified with organosilane groups by Raman Spectroscopy", Ceram. Int., 43 (15), 11838–11847.

[121] Shrivastava A., Gupta V., (2011), "Methods for the determination of limit of detection and limit of quantitation of the analytical methods", Chronicles Young Sci., 2 (1), 21.

[122] Hegnerová K., Piliarik M., Šteinbachová M., Flegelová Z., Černohorská H., Homola J., (2010), "Detection of bisphenol A using a novel surface plasmon resonance biosensor", Anal. Bioanal. Chem., 398 (5), 1963–1966.

[123] Hegnerová K., Homola J., (2010), "Surface plasmon resonance sensor for detection of bisphenol A in drinking water", Sensors Actuators, B Chem., 151 (1), 177–179.

[124] Rodriguez-Mozaz S., De Alda M. L., Barceló D., (2005), "Analysis of bisphenol A in natural waters by means of an optical immunosensor", Water Res., 39 (20), 5071–5079.

[125] Oral A. Y., Bahşi Z. B., Aslan M. H., (2007), "Microstructure and optical properties of nanocrystalline ZnO and ZnO:(Li or Al) thin films", Appl. Surf. Sci., 253 (10), 4593–4598.

BIOGRAPHY

Gamze Sekicek achieved her bachelor's degree from the Department of Biomedical Engineering, at Karabuk University in 2018. She started master's degree program in the Institute of Biotechnology at Gebze Technical University in 2018 fall. Also, she is a research assistant at same Institute. She presented a poster in the International Conference on Nanomaterials, Nanofabrication and Nanocharacterization (NANOMACH) 2020 namely "Microstructural Properties of Ca Doped ZnO Thin Films". Moreover, she has a research paper namely "Synthesis and characterization of Ca doped ZnO thin films by sol–gel method".